

DETERMINATION OF THE HUBBLE CONSTANT, THE INTRINSIC SCATTER OF LUMINOSITIES OF TYPE Ia SUPERNOVAE, AND EVIDENCE FOR NONSTANDARD DUST IN OTHER GALAXIES

XIAOFENG WANG,^{1,2,3} LIFAN WANG,⁴ REYNALD PAIN,³ XU ZHOU,² AND ZONGWEI LI⁵

Received 2005 November 21; accepted 2006 March 15

ABSTRACT

A sample of 109 Type Ia supernovae (SNe Ia) with recession velocity $\lesssim 30,000$ km s⁻¹ is compiled from published SN Ia light curves to explore the expansion rate of the local universe. Based on the color parameter ΔC_{12} and the decline rate Δm_{15} , we found that the average absorption-to-reddening ratios for SN Ia host galaxies are $R_{UBVI} = 4.37 \pm 0.25$, 3.33 ± 0.11 , 2.30 ± 0.11 , and 1.18 ± 0.11 , which are systematically lower than the standard values in the Galaxy. We investigated the correlations of the intrinsic luminosity with light-curve decline rate, color index, and SN environmental parameters. In particular, we found that SNe Ia in E/S0 galaxies close to the central region are brighter than those in the outer region, which may suggest a possible metallicity effect on SN luminosity. The dependence of SN luminosity on galactic environment disappears after corrections for the extinction and ΔC_{12} . The Hubble diagrams constructed using 73 Hubble flow SNe Ia yield a 1σ scatter of $\lesssim 0.12$ mag in *BVI* bands and ~ 0.16 mag in *U* band. The luminosity difference between normal SNe Ia and peculiar objects (including SN 1991bg-like and SN 1991T-like events) has now been reduced to within 0.15 mag via ΔC_{12} correction. We use the same precepts to correct the nearby SNe Ia with Cepheid distances and found that the fully corrected absolute magnitudes of SNe Ia are $M_B = -19.33 \pm 0.06$ and $M_V = -19.27 \pm 0.05$. We deduced a value for the Hubble constant of $H_0 = 72 \pm 6$ (total) km s⁻¹ Mpc⁻¹.

Subject headings: Cepheids — cosmological parameters — cosmology: observations — distance scale — dust, extinction — supernovae: general

1. INTRODUCTION

Type Ia supernovae (SNe Ia) are probably the most precise distance indicators known for measuring the extragalactic distances. Their Hubble diagram, i.e., magnitude-redshift ($m-z$) relation, can be used to trace the expansion history of the universe. The linear portion of the Hubble diagram with absolute magnitude calibration determines the Hubble constant (see a review in Branch 1998); curvature in the diagram probes evolution of the expansion rate, i.e., acceleration or deceleration, and consequently different combinations of the cosmological parameters such as Ω_m and Ω_Λ (Riess et al. 1998; Perlmutter et al. 1999).

Various empirical methods have been developed to calibrate the peak luminosities of SNe Ia. These include the template fitting or Δm_{15} method (Phillips 1993; Hamuy et al. 1996a; Phillips et al. 1999), the multicolor light-curve shape (MLCS) method (Riess et al. 1996b; Jha 2002), the stretch factor method (Perlmutter et al. 1997; Goldhaber et al. 2001), the “Bayesian template method” (BATM; Tonry et al. 2003), and the recently proposed spectral adaptive light-curve (SALT) method (Guy et al. 2005). These methods are fundamentally identical by utilizing the relationship between SN Ia light-curve shape and peak luminosity. The color-magnitude intercept method (CMAGIC) of Wang et al. (2003, 2006) shows some variance, which replaces the magnitude at maximum with the more uniform magnitude at a given value of the color index. The above methods can yield

distances to SN Ia host galaxies with a relative precision approaching 8%–11%, which demonstrates the power of SNe Ia as cosmological lighthouses for extragalactic distance scales. Wang et al. (2005) recently proposed a method that is similar to the Δm_{15} method of Phillips et al. (1999), but instead of using the $B - V$ color at maximum, we proposed using the $B - V$ color at 12 days past optical maximum as a more efficient calibration parameter.

By common practice so far, the spectroscopically peculiar SNe Ia are usually excluded or given a lower weight in cosmological studies. According to Li et al. (2001a), however, the total rate of peculiar SNe Ia in a volume-limited search could be as high as 36%. The rate of SN 1991T/SN 1999aa-like objects is $\sim 20\%$ and the rate of SN 1991bg-like objects is $\sim 16\%$. Some of the peculiar SNe Ia apparently deviate from the relation between light-curve shape and luminosity. The ΔC_{12} method provides a better way to homogenize the normal SNe Ia and the spectroscopically peculiar ones in a more unified and consistent manner.

The color parameter $\Delta C_{12} = (B - V)_{12}$ gives tighter empirical relations with SN Ia peak luminosities (Wang et al. 2005). Here we apply this method to study the local Hubble diagram by including different peculiar types of SNe Ia. Based on the Hubble flow SNe Ia and nearby ones with Cepheid distances, we deduce the value of the Hubble constant. In § 2 we describe the data selection for this study. In § 3 we derive the host galaxy reddening of SNe Ia and estimate the ratios of extinction to reddening for dust in SN host galaxies. In § 4 we examine the luminosity dependence of SNe Ia on secondary parameters. In § 5 we present the Hubble diagram of SNe Ia and give the best estimates of H_0 . Conclusions and discussion are given in § 6.

2. THE DATA

The major sources of SN Ia light curves are (1) the *BVI* light curves of 29 SNe Ia from the earlier Calan/Tololo SN survey (CTIO sample; see Hamuy et al. 1996a, 1996b, 1996c), (2) the

¹ Physics Department and Tsinghua Center for Astrophysics (THCA), Tsinghua University, Beijing 100084, China; wang_xf@mail.tsinghua.edu.cn.

² National Astronomical Observatories of China, Chinese Academy of Sciences, A20 Datun Road, Chaoyang Beijing 100012, China; wxf@vega.bac.pku.edu.cn.

³ Laboratoire de Physique Nucléaire et de Hautes Energies, CNRS-IN2P3, University of Paris VI and VII, Paris, France.

⁴ Lawrence Berkeley National Laboratory, 1 Cyclotron Road, Berkeley, CA 94720.

⁵ Department of Astronomy, Beijing Normal University, 19 Xingjiekouwai Daijie, Beijing 100875, China.

BVRI light curves of 22 SNe Ia collected by the CfA (CfA I sample; see Riess et al. 1999), (3) the *UBVRI* light curves of another 44 SNe Ia from the CfA SN monitoring campaign (CfA II sample; see Jha et al. 2006b), and (4) the Las Campanas/CTIO observing campaign, which covers broadband *UBVRIJHK* photometry (Krisciunas et al. 2001, 2003, 2004a, 2004b).

Reindl et al. (2005; hereafter R05) compiled a sample of 124 nearby SNe Ia ($z \lesssim 0.1$). Our sample is different in that we include only SNe with CCD measurements and those observed 8 days before maximum and with more than five photometric points. The sample includes 109 SNe Ia, 88 of which are spectroscopically normal (Branch et al. 1993), 13 are SN 1991T/SN 1999aa-like (Phillips et al. 1992; Fillipenko et al. 1992b; Li et al. 2001a), and 6 are SN 1991bg-like (Fillipenko et al. 1992a; Leibundgut et al. 1993). For light-curve fitting, we follow the template fitting procedure of Hamuy et al. (1996c) but with six additional template SNe for better Δm_{15} sampling. Besides the SN templates (viz., SN 1991T, SN 1992bc, SN 1992al, SN 1992A, SN 1992bo, SN 1991bg) initially used by Hamuy et al. (1996c), six additional SNe are included as templates: SN 1999aa ($\Delta m_{15} = 0.82$), SN 1999ee ($\Delta m_{15} = 0.95$), SN 1998aq–SN 1998bu ($\Delta m_{15} = 1.05$), SN 1996X–SN 2002er ($\Delta m_{15} = 1.32$), SN 2000dk ($\Delta m_{15} = 1.62$), and SN 1999by ($\Delta m_{15} = 1.90$). These light-curve templates were also used to derive the peak magnitudes in the *U* band. Table 1 shows the fitted parameters for this sample. They are tabulated in the following manner: Column (1) gives the name of each SN. Column (2) gives the name of the corresponding host galaxy. Column (3) gives the redshift in the reference frame of the cosmic microwave background (CMB), using the procedure given at the NASA Extragalactic Database⁶ (NED) or for a self-consistent Virgocentric infall vector of 220 km s^{-1} taken from R05. Columns (4)–(7) give the fitted peak magnitudes in *UBVI* bands, corrected for the Galactic reddening from Schlegel et al. (1998) and the *K*-corrections from Nugent et al. (2002). The magnitude errors in units of 0.01 mag were a quadrature sum of the uncertainties in the observed magnitudes, foreground reddening (0.08 mag in *U*, 0.06 mag in *B*, 0.045 mag in *V*, and 0.03 mag in *I*), and the *K* term (assumed to be 0.02 mag). Column (8) gives the decline rate Δm_{15} , corrected for the small reddening effect (Phillips et al. 1999). Column (9) gives the $B - V$ color 12 days after *B* maximum. It was measured directly from the photometry or from the best-fit light-curve template when the observed color curves were too sparse to be measured accurately. The ΔC_{12} value presented here was already corrected for Galactic reddening. Column (10) gives the Galactic reddening following Schlegel et al. (1998). Column (11) gives the reddening $E(B - V)$ in the host galaxy as derived from the tail of the $B - V$ color curves (Phillips et al. 1999; Altavilla et al. 2004). Column (12) gives the reddening $E(B - V)$ in the host galaxy as determined from the postmaximum color ΔC_{12} (see § 3 and Wang et al. 2005). Column (13) gives the adopted reddening $E(B - V)_{\text{host}}$ in the host galaxy, which is the weighted average of columns (11) and (12). Column (14) gives the key reference sources of SN Ia photometry.

In Table 2, additional information is assembled for the corresponding host galaxies of the SNe Ia listed in Table 1. Columns (1)–(3) are self-explanatory. Columns (4) and (5) list the morphological and coded Hubble types of the host galaxies. Column (6) gives the deprojected galactocentric distances of the SNe in their respective host galaxies in units of the galaxy radius r_{25} (taken from the work of B. Xu & X. F. Wang 2006, in preparation). Columns (7)–(10) give the luminosity distances to the SNe Ia (see discussion in § 5.3).

3. THE EXTINCTION CORRECTION

The Galactic extinction is corrected by using the dust maps from Schlegel et al. (1998). We need to know the intrinsic colors of SNe to estimate the reddening by the dust in the host galaxies. This unavoidably requires assumptions on the intrinsic properties of SNe.

3.1. The Colors and Reddening of SNe Ia

It was shown by Lira (1995) that the intrinsic $B - V$ color evolution of SNe Ia 30–90 days past *V* maximum can be well approximated by a simple linear relation: $(B - V)_0 = 0.725 - 0.0118(t_V - 60)$, where t_V is the time (in days) from the *V* maximum. By empirically assuming that the intrinsic colors of SNe at late time are all identical and follow the above relation, one can deduce the reddening from the offset of the observed “tail” color of SNe Ia from the above relation. The host galaxy reddening $E(B - V)_{\text{tail}}$ estimated this way is reported in column (11) of Table 1.

The tail color is difficult to measure accurately. In most cases, we have to use the colors at maximum or shortly after maximum, provided that their intrinsic behavior is understood. It is difficult to define a reddening-free sample of SNe. Therefore, we have applied a color cut of $E(B - V)_{\text{tail}} \lesssim 0.06$ mag to construct a subsample of 36 SNe, which are likely to suffer little absorption. Figure 1 shows Δm_{15} dependence of the peak colors $U_{\text{max}} - B_{\text{max}}$, $B_{\text{max}} - V_{\text{max}}$, $V_{\text{max}} - I_{\text{max}}$, and the postmaximum color ΔC_{12} . Half of these SNe are located in the dust-poor earlier type E/S0 galaxies. A total of 80% of the remaining half are located in the outskirts of their spiral hosts.

As shown in Figure 1, all colors show similar “kinks” near $\Delta m_{15} \sim 1.65$. A simple linear relation failed to describe the color- Δm_{15} relation for these SNe Ia. A cubic spline is employed to fit the data points in Figure 1. This results in a dispersion of 0.07–0.08 mag for *BVI* colors at maximum. The peak $U - B$ color shows a wider range (from about -0.6 to 0.6) for SNe with different Δm_{15} . The scatter in the $U - B$ color is also larger, e.g., ~ 0.14 mag (for a similar argument by using the stretch factor see Jha et al. 2006b).

Compared to the *UBVI* colors at maximum light, the postmaximum color parameter ΔC_{12} shows a much tighter dependence on Δm_{15} , which is given as

$$\begin{aligned} \Delta C_{12} = & 0.33_{\pm 0.01} + 0.32_{\pm 0.04}(\Delta m_{15} - 1.1) \\ & - 0.56_{\pm 0.21}(\Delta m_{15} - 1.1)^2 + 2.16_{\pm 0.22}(\Delta m_{15} - 1.1)^3, \\ \sigma = & 0.043. \end{aligned} \quad (1)$$

The dispersion of ~ 0.04 mag is comparable to the intrinsic dispersion of the evolution of the tail color (e.g., Lira 1995; Phillips et al. 1999) and is much less than that of the peak color- Δm_{15} relation. The residual distribution for the fit to the color- Δm_{15} correlation, as shown in Figure 2, reveals that the larger scatter of the peak colors is not due to individual observations but tends to be an overall behavior.

Theoretically, the SN colors are related to the exact changes of the optical depth in the ejecta. The peak colors of SNe Ia show very rapid evolution, and small measurement errors may result in systematically incorrect reddening measurements (Leibundgut 2000). For these reasons, we would prefer to use the postmaximum color ΔC_{12} as an alternative reddening indicator. Remember that equation (1) is derived from SNe Ia with $0.8 < \Delta m_{15} < 2.0$, and it may not apply to those SNe Ia with decline rates beyond the above range (e.g., SN 2001ay, which has the broadest

⁶ See <http://nedwww.ipac.caltech.edu>.

TABLE 1
PARAMETERS OF WELL-OBSERVED NEARBY SNe Ia

SN (1)	GALAXY (2)	$v_{\text{CMB}/220}$ (3)	U_{max} (4)	B_{max} (5)	V_{max} (6)	I_{max} (7)	Δm_{15} (8)	ΔC_{12} (9)	$E(B - V)$				REFERENCES (14)
									Galactic (10)	Tail (11)	ΔC_{12} (12)	Host (13)	
1937C.....	IC 4182	330	...	8.74(09)	8.77(11)	...	0.87(10)	0.21(05)	0.014	0.04(05)	0.03(06)	0.04(04)	1, 2
1972E.....	NGC 5253	167	7.44(20)	8.11(10)	8.17(09)	...	0.87(10)	0.24(05)	0.056	0.05(05)	0.06(06)	0.05(04)	3
1974G.....	NGC 4414	655	...	12.45(16)	12.34(19)	...	1.03(10)	0.47(07)	0.018	0.07(17)	0.17(08)	0.15(07)	4
1981B.....	NGC 4536	1179	11.72(12)	11.96(08)	11.92(07)	...	1.11(07)	0.47(05)	0.018	0.10(14)	0.13(06)	0.12(05)	5
1986G.....	NGC 5128	317	12.57(12)	11.95(08)	11.07(07)	...	1.73(05)	1.49(05)	0.115	0.54(06)	0.60(06)	0.57(04)	6, 7
1989B.....	NGC 3627	549	12.15(11)	12.20(07)	11.88(06)	11.64(06)	1.35(05)	0.82(04)	0.032	0.48(16)	0.41(06)	0.42(06)	8
1990N.....	NGC 4639	1179	12.24(09)	12.64(07)	12.64(05)	12.89(04)	1.06(03)	0.36(02)	0.026	0.16(05)	0.05(05)	0.11(04)	9
1990O.....	MCG +3-44-03	9175	...	16.19(10)	16.22(08)	16.56(09)	0.96(10)	0.32(03)	0.093	0.07(06)	0.05(05)	0.05(04)	10
1990af.....	Anon 213562	14966	...	17.77(07)	17.75(06)	...	1.62(05)	0.62(04)	0.035	0.00(10)	-0.03(06)	0.00(04)	10
1991T ^a	NGC 4527	1179	11.16(09)	11.60(07)	11.44(06)	11.63(05)	0.95(05)	0.48(05)	0.022	0.15(05)	0.22(06)	0.18(04)	9
1991ag.....	IC 4919	4161	...	14.35(14)	14.36(16)	14.68(16)	0.88(10)	0.22(05)	0.062	0.09(07)	0.01(07)	0.05(05)	10
1991bg ¹	NGC 4374	1179	...	14.58(08)	13.83(07)	13.43(06)	1.93(05)	1.51(08)	0.040	0.00(09)	0.06(08)	0.04(07)	10
1992A.....	NGC 1992A	1338	...	12.50(07)	12.50(07)	12.77(06)	1.47(05)	0.51(03)	0.018	0.00(03)	0.02(04)	0.02(03)	10, 11
1992P.....	IC 3690	7939	...	16.05(07)	16.09(06)	16.38(08)	0.86(10)	0.22(03)	0.021	0.10(05)	0.03(05)	0.07(04)	10
1992ae.....	Anon 2128-61	22366	...	18.57(10)	18.43(08)	...	1.47(10)	0.51(05)	0.036	0.04(11)	0.03(06)	0.03(05)	10
1992ag.....	ESO 508-G67	8095	...	16.23(08)	16.16(07)	16.38(06)	1.11(10)	0.45(05)	0.097	0.45(20)	0.12(06)	0.15(06)	10
1992al.....	ESO 234-G69	4214	...	14.44(07)	14.54(06)	14.88(06)	1.11(05)	0.31(03)	0.034	0.05(05)	-0.02(05)	0.00(04)	10
1992aq.....	Anon 2304-37	30014	...	19.31(12)	19.29(08)	19.46(12)	1.33(10)	0.49(05)	0.012	0.03(26)	0.09(07)	0.09(07)	10
1992bc.....	ESO 300-G9	5876	...	15.04(07)	15.17(06)	15.51(05)	0.87(05)	0.12(03)	0.022	-0.03(05)	-0.07(05)	0.00(04)	10
1992bg.....	Anon 0741-62	10936	...	16.59(08)	16.67(07)	16.98(06)	1.09(10)	0.29(04)	0.185	0.05(05)	-0.03(06)	0.01(04)	10
1992bh.....	Anon 0459-58	13519	...	17.64(08)	17.53(06)	17.71(07)	1.07(10)	0.51(05)	0.022	0.12(08)	0.19(07)	0.18(05)	10
1992bk.....	ESO 156-G8	17237	...	18.01(12)	18.05(12)	18.24(11)	1.60(10)	0.62(08)	0.015	-0.01(10)	-0.01(09)	0.00(05)	10
1992bl.....	ESO 291-G11	12661	...	17.30(08)	17.32(07)	17.57(06)	1.49(10)	0.51(05)	0.011	0.04(06)	0.02(07)	0.03(04)	10
1992bo.....	ESO 352-G57	5445	...	15.74(07)	15.76(06)	15.92(05)	1.69(05)	0.70(03)	0.027	-0.01(12)	-0.07(05)	0.00(05)	10
1992bp.....	Anon 0336-18	23557	...	18.29(07)	18.30(06)	18.58(07)	1.32(10)	0.38(06)	0.069	0.01(21)	-0.00(07)	0.00(07)	10
1992br.....	Anon 0145-56	26259	...	19.31(17)	19.19(10)	...	1.66(10)	0.71(06)	0.026	0.03(23)	-0.01(08)	0.00(08)	10
1992bs.....	Anon 0329-37	18787	...	18.33(09)	18.25(07)	...	1.34(10)	0.50(04)	0.011	0.07(10)	0.10(06)	0.09(05)	10
1993B.....	Anon 1034-34	21011	...	18.37(11)	18.39(09)	18.55(11)	1.20(10)	0.46(05)	0.079	0.27(18)	0.11(07)	0.12(07)	10
1993H.....	ESO 445-G66	7523	...	16.73(07)	16.52(06)	16.51(06)	1.69(10)	0.82(05)	0.060	0.06(05)	0.04(07)	0.05(04)	10
1993O.....	Anon 1331-33	15867	...	17.56(07)	17.66(06)	17.89(06)	1.33(05)	0.41(03)	0.053	0.05(07)	0.02(05)	0.03(04)	10
1993ac.....	PGC 17787	14674	...	17.75(16)	17.71(12)	17.83(11)	1.45(10)	0.55(06)	0.163	-0.02(10)	0.09(07)	0.05(06)	12
1993ag.....	Anon 1003-35	15013	...	17.81(08)	17.73(06)	18.03(06)	1.36(10)	0.57(05)	0.112	0.12(08)	0.16(07)	0.14(05)	10
1994D.....	NGC 4526	1179	11.18(09)	11.75(07)	11.83(06)	12.11(05)	1.27(05)	0.34(03)	0.022	0.05(08)	-0.03(05)	0.00(04)	13, 14
1994M.....	NGC 4493	7289	...	16.24(08)	16.22(07)	16.35(06)	1.44(10)	0.54(04)	0.023	0.13(06)	0.07(06)	0.10(04)	12
1994S.....	NGC 4495	4829	...	14.71(07)	14.77(06)	15.08(06)	1.02(10)	0.26(05)	0.021	0.00(10)	0.04(07)	0.00(07)	12
1994T.....	PGC 46640	10703	...	17.34(09)	17.16(08)	17.35(07)	1.55(10)	0.69(10)	0.029	0.07(20)	0.13(07)	0.12(07)	12
1994ae.....	NGC 3370	1575	12.28(12)	12.89(07)	12.94(06)	13.25(05)	0.89(05)	0.22(02)	0.031	0.03(05)	0.00(05)	0.02(04)	15
1995D.....	NGC 2962	2129	...	13.18(07)	13.23(06)	13.58(05)	1.00(05)	0.31(03)	0.058	0.09(05)	0.02(05)	0.06(03)	12
1995E.....	NGC 2441	3510	...	16.70(07)	16.01(06)	15.28(05)	1.15(05)	1.09(05)	0.027	0.73(15)	0.74(07)	0.74(06)	12
1995ac ^a	Anon 2245-08	14635	...	17.04(07)	17.07(06)	17.28(06)	0.91(05)	0.21(05)	0.042	0.04(07)	-0.03(06)	0.00(05)	12
1995al.....	NGC 3021	1851	...	13.26(07)	13.22(06)	13.50(05)	0.95(05)	0.37(03)	0.014	0.18(05)	0.12(05)	0.15(04)	12
1995ak.....	IC 1844	6589	...	16.00(08)	15.91(09)	16.12(09)	1.35(10)	0.51(03)	0.038	0.20(12)	0.10(05)	0.11(05)	12
1995bd ^a	UGC 3151	4326	...	15.16(07)	14.92(06)	15.03(06)	1.01(05)	0.54(03)	0.498	0.18(05)	0.24(05)	0.21(04)	12
1996C.....	MCG +8-25-47	9036	...	16.48(10)	16.49(10)	16.65(08)	0.94(10)	0.34(05)	0.013	0.08(06)	0.09(07)	0.08(05)	12
1996X.....	NGC 5061	2120	...	12.96(07)	12.97(06)	13.23(05)	1.33(05)	0.44(02)	0.069	0.06(05)	0.04(04)	0.05(03)	12, 16
1996Z.....	NGC 2935	2285	...	14.32(07)	14.00(06)	...	1.06(10)	0.68(05)	0.064	...	0.37(06)	0.37(06)	12
1996ab.....	Anon 1521+28	37370	...	19.54(09)	19.43(08)	...	1.16(05)	0.38(10)	0.032	0.03(08)	0.04(10)	0.03(07)	12
1996ai.....	NGC 5005	1298	...	16.90(08)	15.17(09)	13.93(10)	1.02(10)	1.92(05)	0.014	2.03(14)	1.63(06)	1.69(06)	12
1996bk.....	NGC 5308	2462	...	14.70(09)	14.40(11)	14.26(08)	1.69(10)	1.00(07)	0.018	0.31(13)	0.23(08)	0.26(07)	12
1996bl.....	Anon 0036+11	10447	...	16.68(07)	16.68(07)	16.87(07)	1.11(10)	0.36(04)	0.092	0.13(07)	0.03(06)	0.07(04)	12
1996bo.....	NGC 673	4898	...	15.82(07)	15.53(06)	15.52(06)	1.30(05)	0.72(03)	0.077	0.30(10)	0.34(05)	0.33(04)	11, 12
1996bv.....	UGC 3432	5016	...	15.34(13)	15.14(10)	15.35(09)	0.95(10)	0.44(06)	0.105	0.21(10)	0.18(07)	0.19(05)	12
1997E.....	NGC 2258	3998	14.74(09)	15.05(08)	15.02(07)	15.17(06)	1.44(05)	0.56(05)	0.124	0.07(05)	0.10(06)	0.08(04)	17
1997Y.....	NGC 4675	4968	14.82(10)	15.26(08)	15.24(08)	15.38(06)	1.26(10)	0.47(05)	0.017	0.08(05)	0.10(06)	0.09(04)	17
1997bp.....	NGC 4680	2647	13.84(09)	13.89(07)	13.72(06)	14.03(05)	1.19(06)	0.58(05)	0.044	0.14(05)	0.22(07)	0.17(04)	11, 17
1997bq.....	NGC 3147	2879	14.10(10)	14.44(11)	14.24(08)	14.39(10)	1.11(10)	0.54(05)	0.032	0.17(05)	0.24(07)	0.19(04)	17
1997br ^a	ESO 579-G40	2193	13.00(15)	13.61(10)	13.40(08)	13.42(20)	1.15(10)	0.75(03)	0.113	0.31(05)	0.41(05)	0.36(04)	17, 18
1997cn ^b	NGC 5490	5246	16.89(20)	16.89(15)	16.35(10)	16.21(10)	1.88(10)	1.28(06)	0.027	0.06(13)	0.00(07)	0.01(06)	17, 19
1997dg.....	Anonymous	9845	16.31(10)	16.83(07)	16.84(07)	16.92(06)	1.19(10)	0.44(05)	0.078	0.29(20)	0.10(06)	0.12(07)	17
1997do.....	UGC 3845	3135	14.00(15)	14.32(11)	14.28(07)	14.52(07)	0.99(10)	0.40(06)	0.063	0.16(08)	0.12(08)	0.14(06)	17
1998V.....	NGC 6627	5161	14.53(10)	15.06(08)	15.05(07)	15.27(06)	1.08(10)	0.35(04)	0.196	0.08(05)	0.03(06)	0.06(04)	17
1998ab ^a	NGC 4704	8354	15.59(12)	16.05(09)	16.06(08)	16.29(08)	1.12(10)	0.39(03)	0.017	0.18(07)	0.06(05)	0.09(04)	17

TABLE 1—Continued

SN (1)	GALAXY (2)	$v_{\text{CMB}/220}$ (3)	U_{max} (4)	B_{max} (5)	V_{max} (6)	I_{max} (7)	Δm_{15} (8)	ΔC_{12} (9)	$E(B - V)$				REFERENCES (14)
									Galactic (10)	Tail (11)	ΔC_{12} (12)	Host (13)	
1998aq.....	NGC 3982	1514	11.63(09)	12.30(07)	12.41(06)	12.69(05)	1.05(03)	0.28(03)	0.014	-0.03(05)	0.07(04)	0.03(04)	17
1998bp ^b	NGC 6495	3048	15.21(10)	15.32(10)	15.02(08)	14.91(08)	1.83(05)	1.06(05)	0.076	0.06(05)	-0.03(07)	0.02(04)	17
1998bu.....	NGC 3368	810	11.77(09)	12.11(07)	11.80(06)	11.59(05)	1.02(03)	0.64(03)	0.025	0.37(05)	0.34(05)	0.36(04)	17
1998de ^b	NGC 252	4713	17.90(20)	17.31(07)	16.63(06)	16.48(08)	1.95(09)	1.58(06)	0.058	0.00(10)	0.03(07)	0.02(06)	17, 20
1998dh.....	NGC 7541	2766	13.53(20)	13.81(08)	13.74(07)	13.92(07)	1.28(10)	0.53(06)	0.068	0.15(05)	0.15(07)	0.15(04)	17
1998dx.....	UGC 11149	14895	17.03(16)	17.53(12)	17.64(10)	17.75(09)	1.47(10)	0.43(05)	0.041	-0.04(08)	-0.05(07)	0.00(06)	17
1998eg.....	UGC 12133	7067	15.63(16)	16.07(07)	16.07(06)	16.24(06)	1.13(05)	0.44(04)	0.123	0.08(10)	0.10(06)	0.09(06)	17
1998es ^a	NGC 632	2872	13.28(09)	13.81(07)	13.73(06)	14.00(05)	0.88(05)	0.33(04)	0.032	0.17(06)	0.12(06)	0.15(05)	17
1999aa ^a	NGC 2595	4572	14.15(09)	14.71(07)	14.73(06)	15.13(05)	0.82(05)	0.19(03)	0.040	0.04(05)	0.05(05)	0.05(04)	17
1999ac ^a	NGC 6063	2950	13.77(09)	14.08(09)	14.05(07)	14.22(06)	1.38(05)	0.58(05)	0.046	0.07(07)	0.16(07)	0.12(06)	17, 21
1999aw ^a	Anon 1101-06	12363	...	16.72(07)	16.70(06)	17.17(05)	0.81(03)	0.16(03)	0.032	0.00(10)	0.02(05)	0.02(05)	17, 22
1999by ^b	NGC 2841	896	13.73(09)	13.59(07)	13.10(06)	12.88(05)	1.90(05)	1.29(06)	0.016	0.00(04)	-0.06(07)	0.00(03)	17, 23
1999cc.....	NGC 6038	9461	16.56(10)	16.77(10)	16.74(09)	16.88(09)	1.45(10)	0.54(04)	0.023	0.02(06)	0.07(06)	0.05(04)	17, 24
1999cl.....	NGC 4501	1179	15.57(10)	14.86(12)	13.73(08)	13.00(07)	1.29(10)	1.55(06)	0.038	1.24(06)	1.16(07)	1.20(05)	17, 24
1999cp.....	NGC 5468	3109	...	13.94(09)	13.96(08)	14.19(07)	1.05(10)	0.34(06)	0.024	...	0.03(07)	0.03(07)	17
1999da ^b	NGC 6411	3644	...	16.61(09)	16.03(09)	15.73(08)	1.94(10)	1.46(06)	0.058	0.05(20)	-0.04(08)	0.00(07)	24
1999dk.....	UGC 1087	4184	14.47(13)	14.81(09)	14.76(07)	15.10(06)	0.99(10)	0.41(05)	0.054	0.15(21)	0.13(07)	0.13(06)	11, 24
1999dq ^a	NGC 976	4066	13.86(09)	14.41(07)	14.33(06)	14.57(05)	0.95(05)	0.34(05)	0.110	0.15(07)	0.08(06)	0.11(05)	11, 17
1999ee.....	IC 5179	3153	14.63(09)	14.84(07)	14.54(06)	14.62(05)	0.94(05)	0.54(03)	0.020	0.38(06)	0.29(05)	0.33(04)	24, 25
1999ej.....	NGC 495	3839	14.98(20)	15.30(09)	15.37(07)	15.53(06)	1.39(10)	0.47(05)	0.072	-0.02(17)	0.04(07)	0.02(06)	17
1999ek.....	UGC 3329	5271	...	15.53(07)	15.42(05)	15.53(05)	1.13(03)	0.49(03)	0.553	0.20(08)	0.16(05)	0.17(04)	17, 24
1999gd.....	NGC 2623	5761	16.82(16)	16.88(08)	16.47(07)	16.19(08)	1.13(10)	0.82(06)	0.041	0.45(16)	0.48(07)	0.48(06)	17
1999gh.....	NGC 2986	2314	13.88(20)	14.21(16)	14.13(12)	14.13(10)	1.69(10)	0.86(06)	0.059	0.07(05)	0.08(07)	0.07(04)	17
1999gp ^a	UGC 1993	7811	15.47(10)	16.01(08)	15.95(07)	16.23(06)	0.92(10)	0.33(05)	0.056	0.11(10)	0.09(07)	0.10(06)	17
2000E.....	NGC 6951	1824	12.50(10)	12.72(07)	12.63(06)	12.77(07)	0.96(05)	0.35(04)	0.366	0.25(10)	0.09(06)	0.13(05)	26
2000bh.....	ESO 573-G014	7238	...	15.86(08)	15.89(07)	16.24(05)	1.16(10)	0.42(05)	0.048	0.07(06)	0.08(07)	0.07(05)	17
2000ca.....	ESO 383-G032	7080	14.96(10)	15.53(07)	15.62(06)	15.93(05)	0.96(05)	0.22(03)	0.067	0.02(05)	-0.03(05)	0.00(04)	24
2000ce.....	UGC 4195	4940	16.76(20)	16.99(16)	16.41(16)	16.04(12)	1.00(10)	0.85(06)	0.057	0.73(15)	0.56(07)	0.59(06)	17, 24
2000cf.....	MCG +11-19-25	10805	16.59(12)	17.00(09)	17.02(08)	17.21(07)	1.27(10)	0.44(04)	0.032	0.11(05)	0.06(05)	0.09(04)	17, 24
2000cn.....	UGC 11064	6971	16.47(10)	16.56(08)	16.40(07)	16.57(05)	1.59(10)	0.73(04)	0.057	0.12(06)	0.12(06)	0.12(05)	17
2000cx ^a	NGC 524	2454	12.74(09)	13.06(07)	12.98(06)	13.49(06)	0.93(05)	0.32(05)	0.083	-0.21(05)	0.06(06)	0.00(04)	17, 27
2000dk.....	NGC 382	4929	15.04(09)	15.33(07)	15.34(06)	15.59(05)	1.63(05)	0.67(07)	0.070	-0.03(06)	0.00(08)	0.00(05)	17
2000fa.....	UGC 3770	6526	15.39(20)	15.70(10)	15.72(10)	15.94(08)	0.98(10)	0.35(05)	0.069	0.12(08)	0.08(07)	0.10(06)	17
2001Va.....	NGC3987	4804	...	14.55(12)	14.53(09)	14.82(08)	0.95(05)	0.28(04)	0.020	0.02(10)	0.02(06)	0.02(06)	28
2001ay ^c	IC 4423	9269	...	16.61(07)	16.62(06)	16.67(06)	0.69(05)	0.38(04)	0.019	0.04(05)	29
2001ba.....	MCG -05-28-001	9245	...	16.17(08)	16.27(09)	16.58(07)	0.98(05)	0.27(05)	0.064	-0.01(10)	-0.01(07)	0.00(05)	24
2001bt.....	IC 4830	4332	...	15.25(07)	15.10(05)	15.18(05)	1.28(05)	0.63(03)	0.065	0.26(06)	0.25(05)	0.25(04)	24
2001cn.....	IC 4758	4628	14.99(18)	15.20(07)	15.11(05)	15.21(05)	1.15(05)	0.51(03)	0.059	0.21(07)	0.17(05)	0.18(04)	24
2001cz.....	NGC 4679	4900	...	15.03(07)	14.97(05)	15.14(05)	1.07(03)	0.36(03)	0.092	0.17(06)	0.04(05)	0.09(04)	24
2001el.....	NGC 1448	1030	12.59(09)	12.75(07)	12.68(06)	12.79(06)	1.13(03)	0.58(02)	0.014	0.29(05)	0.24(05)	0.27(04)	24
2002bo.....	NGC 3190	1547	...	13.93(10)	13.50(10)	13.47(10)	1.13(05)	0.74(05)	0.025	0.43(06)	0.40(07)	0.42(05)	30
2002cx ^c	CGCG 044-035	7488	...	17.56(10)	17.46(16)	17.29(10)	1.28(10)	0.60(05)	0.032	0.14(21)	0.20(07)	0.19(07)	27
2002el.....	NGC 6986	7079	...	16.11(07)	16.16(06)	16.37(07)	1.33(05)	0.49(03)	0.085	0.28(18)	0.09(05)	0.10(05)	31
2002er.....	UGC 10743	2652	13.86(09)	14.21(07)	14.07(06)	14.18(07)	1.33(04)	0.59(05)	0.157	0.21(06)	0.19(06)	0.20(06)	32
2002hu.....	MCG +06-06-012	11000	16.42(09)	16.63(07)	16.68(06)	16.93(07)	1.03(05)	0.31(04)	0.044	0.09(05)	0.01(05)	0.05(04)	33
2003du.....	UGC 9391	2008	13.00(09)	13.49(07)	13.61(06)	13.83(07)	1.00(04)	0.22(05)	0.010	0.05(05)	-0.07(06)	0.00(04)	34
2004S.....	MCG -05-16-021	2516	...	14.01(08)	14.02(09)	14.32(10)	1.11(05)	0.40(05)	0.101	0.08(05)	0.07(06)	0.08(04)	35

^a SN 1991T/SN 1999aa-like SNe.

^b SN 1991bg-like SNe.

^c SN 2001ay is the SN Ia with the broadest light curve (Howell & Nugent 2004); SN 2002cx displayed the most unique spectral and photometric features (Li et al. 2003).

REFERENCES.—(1) Schaefer 1994; (2) Pierce & Jacoby 1995; (3) Ardeberg & Groot 1973; (4) Schaefer 1998; (5) Schaefer 1995; (6) Phillips et al. 1987; (7) Cristiani et al. 1992; (8) Wells et al. 1994; (9) Lira et al. 1998; (10) Hamuy et al. 1996b; (11) Altavilla et al. 2004; (12) Riess et al. 1999; (13) Richmond et al. 1995; (14) Patat et al. 1996; (15) Riess et al. 2005; (16) Salvo et al. 2001; (17) Jha et al. 2006b; (18) Li et al. 1999; (19) Turatto et al. 1998; (20) Modjaz et al. 2001; (21) Phillips et al. 2006; (22) Strolger et al. 2002; (23) Garnavich et al. 2004; (24) Krisciunas et al. 2001, 2003, 2004a, 2004b, 2006; (25) Stritzinger et al. 2002; (26) Valentini et al. 2003; (27) Li et al. 2001b, 2003; (28) Vinko et al. 2003; (29) Howell & Nugent 2004; (30) Benetti et al. 2004; (31) from W. Li; (32) Pignata et al. 2004; (33) Sahu et al. 2006; (34) Anupama et al. 2005; (35) Misra et al. 2005.

TABLE 2
PARAMETERS RELEVANT FOR SN HOST GALAXIES

SN (1)	Galaxy (2)	$z_{\text{CMB}/220}$ (3)	Type (4)	T (5)	r_{SN}/r_{25} (6)	μ_U (7)	μ_B (8)	μ_V (9)	μ_I (10)
1937C.....	IC 4182 ^a	0.0011	Sm	9	0.28(03)
1972E.....	NGC 5253 ^a	0.0006	Im	8
1974G.....	NGC 4414 ^a	0.0022	Sc	5	0.55(03)
1981B.....	NGC 4536 ^a	0.0039	Sbc	4	0.70(05)
1986G.....	NGC 5128	0.0011	S0	-2	0.23(02)	28.36(24)	28.20(19)	28.15(17)	...
1989B.....	NGC 3627 ^a	0.0018	Sb	3	0.21(02)
1990N.....	NGC 4639 ^a	0.0499	Sbc	4	0.84(06)
1990O.....	MCG +3-44-03	0.0306	Sa	1	0.82(05)	...	35.43(20)	35.43(18)	35.51(16)
1990af.....	Anon 213562	0.0039	Sa	1	0.00(05)	...	36.50(19)	36.57(17)	...
1991T.....	NGC 4527 ^a	0.0039	Sbc	4	0.61(02)
1991ag.....	IC 4919	0.0039	Sdm	8	0.80(06)	...	33.78(25)	33.72(23)	33.73(21)
1991bg.....	IC 4374	0.0139	E1	-4	0.30(02)	30.29(23)	30.35(19)	30.31(17)	30.40(14)
1992A.....	NGC 1380	0.0045	S0	-2	0.44(03)	...	31.41(17)	31.46(16)	31.54(14)
1992P.....	IC 3690	0.0265	Sb	3	0.89(13)	...	35.46(19)	35.43(17)	35.43(15)
1992ae.....	Anon 2128-61	0.0746	E/S0	-3	0.15(05)	...	37.48(23)	37.39(19)	...
1992ag.....	ESO 508-G67	0.0270	Sbc	4	35.08(27)	35.10(22)	35.18(16)
1992al.....	ESO 234-G69	0.0141	Sc	5	0.42(03)	...	33.77(19)	33.81(17)	33.85(14)
1992aq.....	Anon 2304-37	0.1001	Sa	1	0.38(10)	...	38.17(29)	38.22(22)	38.23(19)
1992bc.....	ESO 300-G9	0.0196	Sab	4	0.80(23)	...	34.74(19)	34.71(17)	34.67(14)
1992bg.....	Anon 0741-62	0.0364	Sa	1	0.18(10)	...	35.94(19)	35.96(17)	35.97(14)
1992bh.....	Anon 0459-58	0.0451	Sbc	4	0.11(02)	...	36.33(22)	36.36(18)	36.45(15)
1992bk.....	ESO 156-G8	0.0575	E/S0	-2	0.87(08)	...	36.74(24)	36.87(21)	36.90(17)
1992bl.....	ESO 291-G11	0.0422	S0/a	1	1.52(07)	...	36.20(19)	36.28(17)	36.33(14)
1992bo.....	ESO 352-G57	0.0181	S0	-2	1.74(19)	...	34.31(22)	34.47(18)	34.50(15)
1992bp.....	Anon 0336-18	0.0785	S0	-2	0.26(04)	...	37.48(27)	37.47(21)	37.48(16)
1992br.....	Anon 0145-56	0.0875	E/S0	-3	1.23(07)	...	37.86(39)	37.88(28)	...
1992bs.....	Anon 0329-37	0.0626	Sb	3	0.94(06)	...	37.17(22)	37.17(18)	...
1993B.....	Anon 1034-34	0.0700	Sb	3	0.29(03)	...	37.24(28)	37.34(22)	37.35(18)
1993H.....	ESO 445-G66	0.0251	Sab	2	0.35(05)	...	35.00(19)	35.01(17)	34.96(14)
1993O.....	Anon 1331-33	0.0529	S0	-2	1.40(40)	...	36.64(19)	36.75(17)	36.75(14)
1993ac.....	PGC 17787	0.0489	E	-3	0.68(10)	...	36.55(28)	36.59(22)	36.55(18)
1993ag.....	Anon 1003-35	0.0500	S0	-2	0.70(18)	...	36.44(22)	36.51(18)	36.71(15)
1994D.....	NGC 4526	0.0243	S0	-2	0.19(01)	30.99(23)	31.02(19)	31.06(17)	31.05(14)
1994M.....	NGC 4493	0.0161	E	-4	0.68(10)	...	34.99(19)	35.07(17)	35.07(14)
1994S.....	NGC 4495	0.0357	Sab	2	0.74(09)	...	34.14(27)	34.11(21)	34.10(16)
1994T.....	PGC 46640	0.0052	Sa	1	35.77(28)	35.78(22)	35.92(16)
1994ae.....	NGC 3370 ^a	0.0039	Sc	5	0.51(04)
1995D.....	NGC 2962	0.0144	S0	-1	1.18(06)	...	32.43(17)	32.45(16)	32.54(14)
1995E.....	NGC 2441	0.0117	Sb	3	0.41(03)	...	33.49(24)	33.52(20)	33.34(15)
1995ac.....	Anon 2245-08	0.0071	Sa	1	36.56(22)	36.48(18)	36.35(15)
1995ak.....	IC 1844	0.0488	Sbc	4	0.37(03)	...	34.79(22)	34.80(19)	34.87(16)
1995al.....	NGC 3021	0.0062	Sbc	4	0.44(05)	...	32.26(19)	32.27(17)	32.38(14)
1995bd.....	UGC 3151	0.0220	Sbc	4	0.79(09)	...	33.75(19)	33.68(17)	33.73(14)
1996C.....	MCG +8-25-47	0.0301	Sa	1	0.42(03)	...	35.64(23)	35.65(20)	35.58(16)
1996X.....	NGC 5061	0.0071	E0	-5	0.57(03)	...	31.97(17)	32.01(16)	32.06(14)
1996Z.....	NGC 2935	0.0076	Sb	3	0.61(03)	...	32.42(24)	32.42(20)	...
1996ai.....	NGC 5005	0.1246	Sbc	4	0.16(01)	...	30.76(25)	30.67(21)	30.99(17)
1996ab.....	Anon 1521+28	0.0043	Sc	5	38.68(28)	38.56(22)	...
1996bk.....	NGC 5308	0.0082	S0	-2	32.33(28)	32.45(23)	32.49(17)
1996bl.....	Anon 0036+11	0.0348	Sc	5	35.82(19)	35.82(17)	35.78(15)
1996bo.....	NGC 673	0.0163	Sc	5	0.13(01)	...	33.90(19)	33.93(17)	34.02(14)
1996bv.....	UGC 3432	0.0167	Scd	6	0.07(01)	...	34.15(24)	34.06(20)	34.16(16)
1997E.....	NGC 2258	0.0133	S0	-2	0.95(27)	33.81(23)	33.77(19)	33.85(17)	33.87(14)
1997Y.....	NGC 4675	0.0166	Sb	3	0.14(02)	34.13(24)	34.15(19)	34.20(18)	34.17(14)
1997bp.....	NGC 4680	0.0088	Sb	3	0.57(08)	32.72(23)	32.46(19)	32.46(17)	32.70(14)
1997bq.....	NGC 3147	0.0096	Sbc	4	0.62(03)	33.05(24)	33.06(21)	33.02(18)	33.10(16)
1997br.....	ESO 576-G40 ^b	0.0073	Sd	7	0.90(06)	31.11(26)	31.59(20)	31.73(18)	31.89(24)
1997cn.....	NGC 5490	0.0175	E	-5	0.22(02)	34.19(35)	34.33(28)	34.21(21)	34.21(17)
1997dg.....	Anonymous	0.0328	Sa	1	...	35.67(34)	35.75(27)	35.83(22)	35.74(16)
1997do.....	UGC 3845	0.0104	Sbc	4	0.12(01)	33.39(33)	33.27(26)	33.29(20)	33.37(16)
1998V.....	NGC 6627	0.0172	Sb	3	0.86(10)	34.21(24)	34.23(19)	34.21(17)	34.19(14)
1998ab.....	NGC 4704	0.0279	Sbc	4	0.51(04)	35.11(24)	35.10(20)	35.14(18)	35.16(15)
1998aq.....	NGC 3982 ^a	0.0050	Sb	3	0.32(02)
1998bp.....	NGC 6495	0.0102	E	-5	0.21(04)	33.08(24)	33.17(20)	33.19(18)	33.13(15)
1998bu.....	NGC 3368 ^a	0.0027	Sab	2	0.24(01)

TABLE 2—Continued

SN (1)	Galaxy (2)	$z_{\text{CMB}/220}$ (3)	Type (4)	T (5)	r_{SN}/r_{25} (6)	μ_U (7)	μ_B (8)	μ_V (9)	μ_I (10)
1998de.....	NGC 252	0.0157	S0	−1	1.60(19)	34.39(35)	34.15(24)	34.05(20)	34.18(16)
1998dh.....	NGC 7541	0.0092	Sbc	4	0.52(02)	32.58(29)	32.50(19)	32.56(17)	32.64(15)
1998dx.....	UGC 11149	0.0496	Sb	3	0.95(05)	36.60(33)	36.63(26)	36.74(21)	36.60(17)
1998eg.....	UGC 12133	0.0236	Sc	6	0.70(07)	35.02(33)	35.02(24)	35.08(20)	35.06(15)
1998es.....	NGC 632	0.0096	S0	−2	0.23(03)	32.86(26)	32.89(22)	32.84(18)	32.92(15)
1999aa.....	NGC 2595	0.0152	Sc	5	0.38(03)	34.27(23)	34.20(19)	34.13(17)	34.21(14)
1999ac.....	NGC 6063	0.0098	Scd	6	0.85(10)	32.74(30)	32.71(25)	32.83(20)	32.90(15)
1999aw.....	Anon 1101−06	0.0412	?	?	36.29(22)	36.15(18)	36.28(15)
1999by.....	NGC 2841 ^a	0.0030	Sb	3	0.66(02)
1999cc.....	NGC 6038	0.0315	Sc	5	0.50(07)	35.75(24)	35.58(20)	35.64(18)	35.61(16)
1999cl.....	NGC 4501 ^b	0.0039	Sb	3	0.30(01)	30.12(27)	30.12(24)	30.18(19)	30.51(15)
1999cp.....	NGC 5468	0.0104	Scd	6	0.72(03)	...	33.17(28)	33.16(22)	33.12(16)
1999da.....	NGC 6411	0.0121	E	−5	1.03(03)	...	33.71(28)	33.64(22)	33.55(17)
1999dk.....	UGC 1087	0.0139	Sc	5	0.64(08)	33.91(32)	33.79(25)	33.79(20)	33.95(15)
1999dq.....	NGC 976	0.0136	Sc	5	0.19(01)	33.48(27)	33.53(22)	33.46(18)	33.49(15)
1999ee.....	IC 5179	0.0105	Sbc	4	0.31(02)	33.34(23)	33.26(19)	33.19(17)	33.30(14)
1999ej.....	NGC 495	0.0128	S0/a	0	0.80(10)	34.41(35)	34.29(25)	34.39(20)	34.34(15)
1999ek.....	UGC 3329	0.0176	Sbc	4	0.70(12)	...	34.27(19)	34.28(16)	34.29(14)
1999gd.....	NGC 2623	0.0192	Sab	2	0.28(04)	34.54(33)	34.55(25)	34.59(20)	34.56(16)
1999gh.....	NGC 2986	0.0077	E	−5	0.57(04)	32.19(29)	32.38(24)	32.55(20)	32.54(16)
1999gp.....	UGC 1993	0.0260	Sb	3	0.28(03)	35.14(31)	35.16(25)	35.11(20)	35.16(15)
2000E.....	NGC 6951	0.0061	Sbc	4	0.25(01)	32.06(27)	31.79(22)	31.73(18)	31.68(15)
2000bh.....	ESO 573-G014	0.0241	Sc	5	0.50(22)	...	34.88(22)	34.94(18)	35.09(15)
2000ca.....	ESO 383-G032	0.0236	Sbc	4	0.25(04)	35.09(24)	35.03(19)	35.02(17)	34.99(14)
2000ce.....	UGC 4195	0.0165	Sb	3	0.51(07)	34.21(35)	34.45(28)	34.40(25)	34.36(18)
2000cf.....	MCG +11-19-25	0.0360	Sbc	4	0.55(25)	35.98(24)	35.95(20)	36.03(18)	36.03(15)
2000cn.....	UGC 11064	0.0232	Scd	6	0.17(03)	35.04(27)	34.91(22)	34.96(18)	35.10(15)
2000cx.....	NGC 524	0.0082	S0	−1	...	32.60(23)	32.37(19)	32.24(17)	32.45(14)
2000dk.....	NGC 382	0.0164	E	−5	0.51(19)	33.98(26)	33.96(22)	34.09(18)	34.20(15)
2000fa.....	UGC 3770	0.0217	Im	10	0.40(09)	35.00(35)	34.81(25)	34.85(21)	34.85(16)
2001V.....	NGC 3987	0.0160	Sb	3	0.96(09)	...	33.92(26)	33.83(21)	33.82(16)
2001ay.....	IC 4423	0.0309	Sbc	4	0.69(10)	...	35.75(22)	35.75(18)	35.56(15)
2001ba.....	MCG −05-28-001	0.0308	Sbc	4	0.85(08)	...	35.58(22)	35.60(19)	35.59(15)
2001bt.....	IC 4830	0.0144	Sbc	4	0.57(05)	...	33.61(19)	33.69(16)	33.78(14)
2001cn.....	IC 4758	0.0154	Sc	5	0.73(08)	34.06(28)	33.91(19)	33.95(16)	33.95(14)
2001cz.....	NGC 4679	0.0163	Sc	4	0.44(04)	...	34.14(19)	34.09(16)	34.04(14)
2001el.....	NGC 1448	0.0034	Scd	6	...	31.30(23)	31.18(19)	31.33(17)	31.44(14)
2002bo.....	NGC 3190	0.0052	Sa	1	0.17(01)	...	31.84(23)	31.79(20)	31.93(17)
2002cx.....	CGCG 044−035	0.0250	?	?	36.06(28)	36.15(26)	35.94(18)
2002el.....	NGC 6986	0.0236	E/S0	−3	0.86(07)	...	34.95(22)	35.08(18)	35.14(15)
2002er.....	UGC 10743	0.0088	Sa	1	0.38(04)	32.67(30)	32.72(24)	32.76(20)	32.83(16)
2002hu.....	MCG +06-06-012	0.0367	Sc	5	1.17(10)	36.22(23)	35.89(19)	35.91(17)	35.89(15)
2003du.....	UGC 9391	0.0067	Sdm	8	0.34(03)	33.13(23)	32.99(19)	33.01(17)	32.89(15)
2004S.....	MCG −05-16-21	0.0084	Sc	5	1.13(05)	...	33.05(19)	33.09(18)	33.19(16)

^a Host galaxies for which a Cepheid distance is available.

^b The dust in ESO 576-G40 and NGC 4501 may be very different from that of the other distant galaxies (see the discussions in the text), so the distance moduli presented here for them may not represent their true distances.

light curve with $\Delta m_{15} = 0.69$; see Howell & Nugent 2004). Deviation of the observed ΔC_{12} from the curve shown in the bottom panel of Figure 1 gives an estimate of the host galaxy reddening $E(B - V)_{12}$, which is listed in column (12) of Table 1. The above determinations of the host galaxy reddening are well consistent with those estimated by the color at the nebular epoch, with an offset of ~ 0.01 mag and a dispersion of ~ 0.04 mag.

The host galaxy reddening $E(B - V)_{\text{host}}$ was taken to be the weighted average of $E(B - V)_{12}$ and $E(B - V)_{\text{tail}}$. In some cases, the formal mean value turns out to be negative; specifically, the $E(B - V)_{\text{host}}$ values were assumed to be zero. This is equivalent to adopting a Bayesian filter with a flat prior distribution for positive $E(B - V)$ and zero for $E(B - V) < 0$ (Riess et al. 1996b). The adopted $E(B - V)_{\text{host}}$ values are listed in column (13) of Table 1.

Figure 3 shows the distribution of the reddening $E(B - V)_{\text{host}}$ in their host galaxies as a function of the normalized distance of the SN within its host galaxy, r_{SN}/r_{25} (see definition in § 4.2). The SNe farther out are found to have lower reddening values than those in the inner regions. The mean $E(B - V)_{\text{host}}$ value for the SNe in E/S0 galaxies is found to be 0.07 ± 0.02 mag. Excluding the largest contributor SN 1986G in reddening, the mean reddening value still remains at a nonnegligible level of ~ 0.05 mag.

We further compared the values of the host galaxy reddening derived in this paper to the corresponding ones given in R05. As shown in the bottom panel of Figure 3, the mean value of R05 appears to be lower than ours by 0.047 ± 0.051 mag. This difference is related to the assumption on the reddening-free SN sample and the approach to estimate the host galaxy reddening. For example, we define a low-reddening sample of SNe Ia using

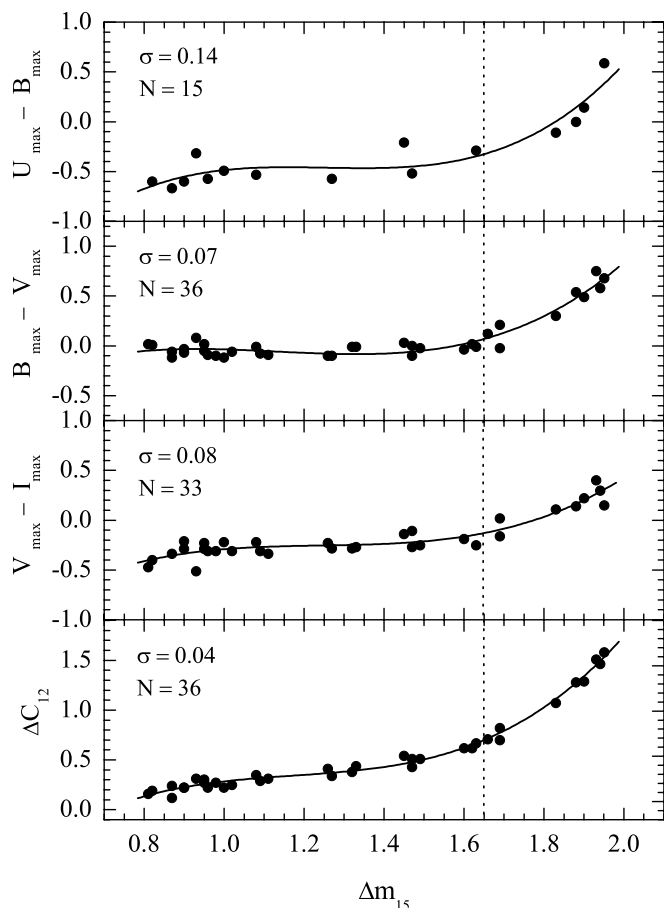


FIG. 1.—Dependence of the color parameters $U_{\max} - B_{\max}$, $B_{\max} - V_{\max}$, $V_{\max} - I_{\max}$, and ΔC_{12} of SNe Ia with negligible host galaxy reddening on the decline rate Δm_{15} .

a color cut of $E(B - V)_{\text{tail}} \lesssim 0.06$ mag, while R05 assumed that all SNe in E/S0 galaxies are free from reddening. According to our analysis, however, the SNe in the E/S0 galaxies may not necessarily guarantee a reddening-free sample.

3.2. Empirical Reddening Relations

An understanding of the reddening relies not only on the availability of independent reddening indicators but also on the specific reddening properties of the dust. The determination of R for the reddening ratios from SNe Ia implies astonishingly different optical properties for dust in distant galaxies. Earlier analysis assuming that SNe Ia have a unique luminosity and color yielded surprising smaller values of $R_B \sim 1.0$ – 2.0 (e.g., Branch & Tammann 1992). Recent determinations of R tend to give more consistent values, e.g., $R_B = 3.55 \pm 0.30$ (Riess et al. 1996a), 3.5 ± 0.4 (Phillips et al. 1999), 3.5 (Altavilla et al. 2004), and 3.65 ± 0.16 (R05). The slight variations among these values are related to the ways of deriving the host galaxy reddening for SNe Ia.

To examine the dust properties of distant galaxies using SNe Ia, it is important to first remove the intrinsic dependence of SN Ia luminosity on the light or color curve parameters. We have shown in Figure 3 of Wang et al. (2005) that the peak luminosities of SNe Ia with minimum absorption can be well calibrated by the color parameter ΔC_{12} . The relation between ΔC_{12} and the absolute magnitudes M in $UBVI$ (which were obtained by assuming $H_0 = 72 \text{ km s}^{-1} \text{ Mpc}^{-1}$), based on a sample of 33 Hubble flow SNe Ia with $E(B - V)_{\text{host}} \lesssim 0.06$ mag as listed in

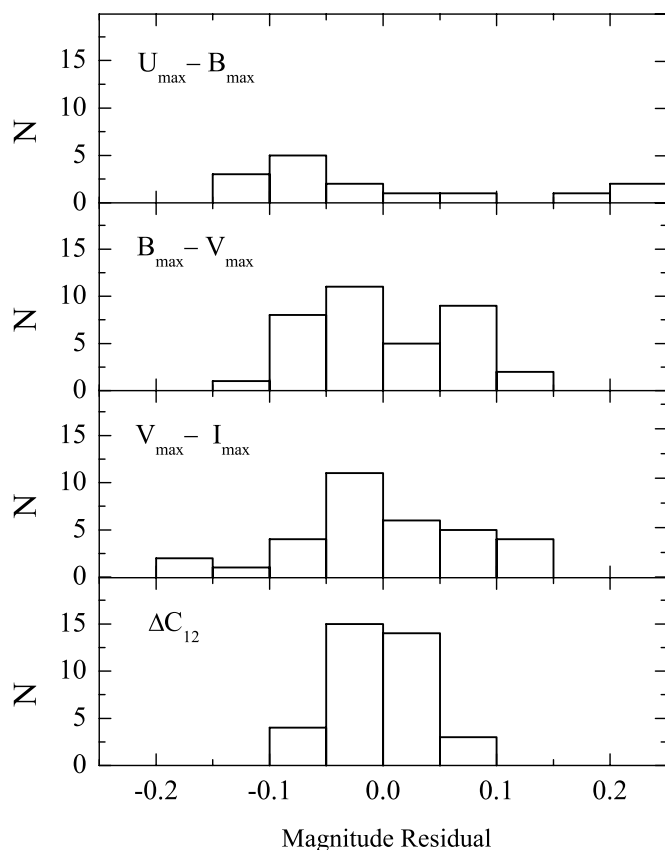


FIG. 2.—Histogram of the residual distribution for the fit to the color- Δm_{15} relation as shown in Fig. 1.

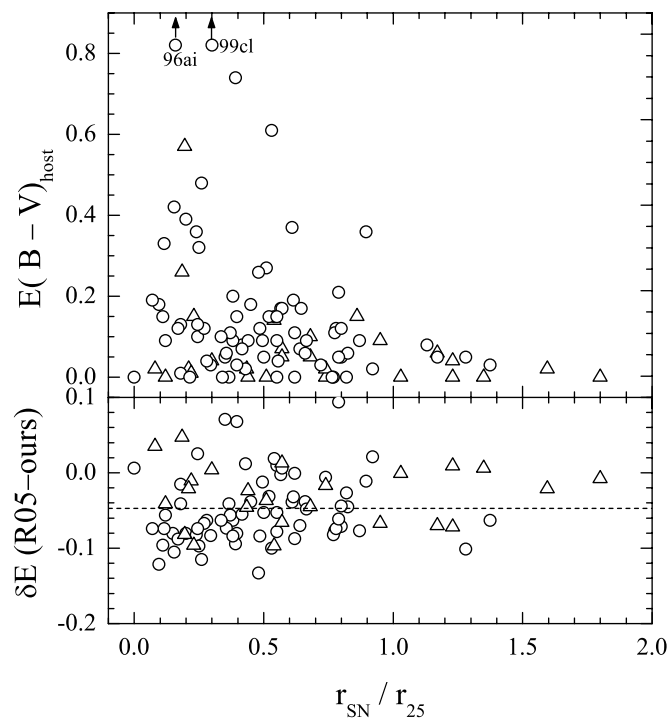


FIG. 3.—*Top*: Reddening distribution of SNe Ia in their respective host galaxies. The circles show the SNe Ia in spiral galaxies, and the triangles represent those in E/S0 galaxies. The two SNe SN 1996ai and SN 1999cl as marked by the arrows have the host galaxy reddening values of $E(B - V)_{\text{host}} = 1.69$ and 1.20 , respectively. *Bottom*: Difference of the host galaxy reddening values as derived between R05 and this paper. The dashed line marks the mean value of the reddening difference.

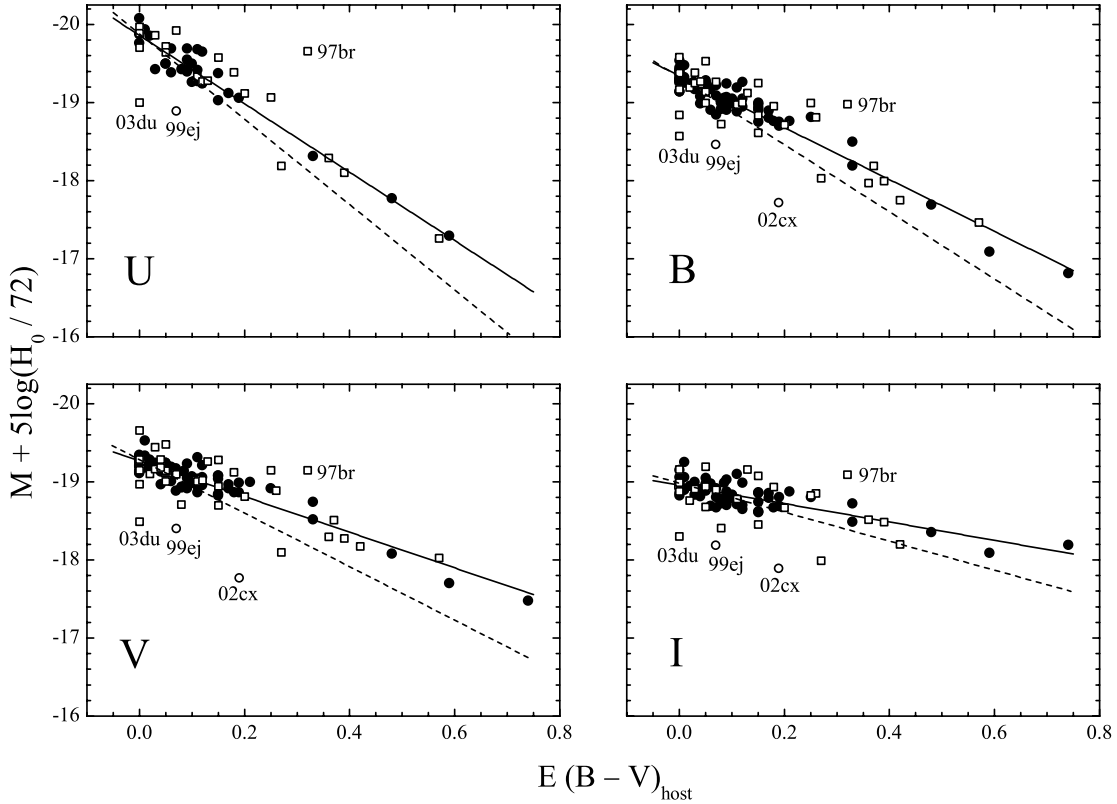


FIG. 4.—Dependence of the absolute magnitudes on the host galaxy reddening $E(B - V)_{\text{host}}$ for SNe Ia in $UBVI$ bands. The absolute magnitudes are corrected for the Galactic absorption and the intrinsic dependence on ΔC_{12} . The circles shown here are the Hubble flow SN sample. The SNe Ia with $v \lesssim 3000 \text{ km s}^{-1}$, represented by squares, are not included in the fits. The two most reddened SNe, SN 1996ai and SN 1999cl, are not shown for the space limit. The solid lines depict the best-fitting reddening vectors in distant galaxies, while the dashed lines show the canonical Galactic reddening vectors.

Table 1 (including four SN 1991T/SN 1999aa–like objects, four SN 1991bg–like objects, and SN 2001ay), can be expressed in terms of linear relations:

$$M_U = -19.75_{\pm 0.09} + 2.55_{\pm 0.15}(\Delta C_{12} - 0.31),$$

$$N = 10, \quad \sigma = 0.202, \quad (2)$$

$$M_B = -19.30_{\pm 0.02} + 1.93_{\pm 0.07}(\Delta C_{12} - 0.31),$$

$$N = 33, \quad \sigma = 0.108, \quad (3)$$

$$M_V = -19.24_{\pm 0.02} + 1.43_{\pm 0.06}(\Delta C_{12} - 0.31),$$

$$N = 33, \quad \sigma = 0.097, \quad (4)$$

$$M_I = -18.97_{\pm 0.02} + 1.01_{\pm 0.06}(\Delta C_{12} - 0.31),$$

$$N = 30, \quad \sigma = 0.101. \quad (5)$$

The normalization to $\Delta C_{12} = 0.31$ corresponds to the color value of the fiducial supernova SN 1992a. The dispersion of the M - ΔC_{12} relation for 24 normal SNe Ia with low dust reddening decreases further down to 0.170 mag in the U band, to 0.069 mag in B band, to 0.068 mag in V band, and to 0.069 mag in I band. Furthermore, the corresponding slopes in $UBVI$ are 1.97 ± 0.52 , 1.72 ± 0.11 , 1.41 ± 0.10 , and 0.96 ± 0.10 , respectively, which are not inconsistent with those shown in the above equations. This demonstrates the robustness of the correlation between the postmaximum color ΔC_{12} and the absolute magnitudes M , in particular in the V and I bands. The larger dispersion in the U band may be caused by small number statistics, the intrinsically larger luminosity dispersion, or both.

The ΔC_{12} procedure thus provides an independent and more precise way to determine the average value of the reddening ratio for distant galaxies hosting SNe Ia. The absolute magnitudes M_{UBVI} of all 109 SNe Ia, corrected for the Galactic extinction and the intrinsic dependence on ΔC_{12} as shown by equations (2)–(5), are plotted against the values of their host galaxy reddening in Figure 4.

SNe shown in Figure 4 with $v \lesssim 3000 \text{ km s}^{-1}$ (*open squares*) were not used for the fit of the reddening vector due to the effect of the peculiar motions of their host galaxies. Moreover, the two Hubble flow events SN 1999ej and SN 2002cx were also not included in the fit. The former is too faint for unknown reasons by about 0.6 mag for a normal SN. The latter is characterized by an SN 1991T–like premaximum spectrum and an SN 1991bg–like luminosity, a normal $B - V$ color evolution, and very low expansion velocities (Li et al. 2003), which may be a new subclass of SNe Ia (Jha et al. 2006a). For the linear fits in Figure 4, the resulting values of R_{UBVI} are

$$R_U = 4.36 \pm 0.25, \quad R_B = 3.33 \pm 0.11,$$

$$R_V = 2.29 \pm 0.11, \quad R_I = 1.18 \pm 0.11, \quad (6)$$

which are clearly smaller than the Galactic values. Our determinations of the R -values are slightly lower than most of the recent determinations. From a sample of 62 Hubble flow SNe Ia, R05 reported recently a value of $R_B = 3.65 \pm 0.16$. Although there were a lot of the same SNe in our analysis, the host galaxy reddening $E(B - V)_{\text{host}}$ we derived for these SNe was different (see § 3.2). The smaller reddening values obtained by R05 consequently led them to derive the larger R -value. Note that they

also derived their $E(B - V)_{\text{host}}$ values from the peak $V - I$ colors, which usually have larger scatter (e.g., 0.08–0.09 mag) and may not be as reliable as a reddening indicator. Very recently, Wang et al. (2006) determined a lower value of $R_B = 2.59 \pm 0.24$ from a combined analysis of the maximum luminosity and the luminosity in the CMAGIC region. This value may parameterize well the effects of both extinction by the host galaxy and intrinsic SN color dependence on luminosity, but not necessarily the true R -value for distant galaxies since they did not try to disentangle these two effects in the analysis. Moreover, their analysis did not include two of the most highly reddened SNe (SN 1995E and SN 1999gd) in the Hubble flow, which may have a significant impact on the final R -values.

The remarkably small scatter associated with the above R_{UBVI} values indicates that the host galaxies for most of the SNe Ia within $z \lesssim 0.1$ do share fairly similar dust properties. Besides the two Hubble flow SNe mentioned above, the highly reddened SN 1999cl (not shown in Fig. 4) is likely to be an outlier, which deviates from the best-fit line by ~ 1.1 mag in B band. The disturbance of the peculiar motion cannot account for the large deviation of SN 1999cl since its host galaxy NGC 4501 (M88) is the member galaxy of the Virgo Cluster. Assuming an average luminosity and a peculiar motion of $< 200 \text{ km s}^{-1}$ for SN 1999cl, one finds $R_B = 2.40 \pm 0.37$ for this individual supernova. This indicates that M88 may have a very nonstandard dust (for an argument of a low $R_V \sim 1.55$ for SN 1999cl see also Krisciunas et al. 2006). SN 1997br, which was a spectroscopically peculiar, SN 1991T-like object (Li et al. 1999), also seems to be an outlier. Applying our R -values to correct the host galaxy extinction of SN 1997br would make it unrealistically bright, in particular in the U band where it is brighter than a normal SN Ia by ~ 1.2 mag. This difference probably suggests a very different dust property for the host galaxy of SN 1997br, ESO 576-G40. However, there is still a large uncertainty in the measurement of the recession velocity of ESO 576-G40 (see discussions in Li et al. 1999), which may also contribute partially to the large deviation of SN 1997br as seen in Figure 4. For the normal and low-reddening SN 2003du (Anupama et al. 2005), a peculiar motion of $\sim 800 \text{ km s}^{-1}$ relative to the CMB frame is needed to explain its “outlying position” in Figure 4.

4. THE LUMINOSITY PROPERTIES OF SNe Ia

Estimates of the host galaxy reddening and determinations of the empirical reddening relations, based on a larger SN Ia sample of different sorts, would enable us to deredden SNe Ia accordingly. This will consequently help to reveal the nature of SNe Ia and to determine the relevant parameters governing their optical properties.

4.1. The Luminosity Diversities

In Figure 5 we plot the distribution of the extinction-corrected absolute magnitudes in $UBVI$ with a bin size of 0.2 mag for all 109 SNe listed in Table 1.

As known in previous studies, different SNe Ia span a wider range over their optical properties (for a review see, e.g., Leibundgut 2000). It is clear from Figure 5 that both the maximum value and the scatter of the luminosity are wavelength dependent. Compared with the luminosity of SNe Ia in the I band, the luminosity in the U band is more luminous and the scatter is also larger. This can be interpreted as that the SN Ia emission in the U band may be more sensitive to the variance of the progenitor properties, such as the metallicity (Hoefflich et al. 1998; Lentz et al. 2000).

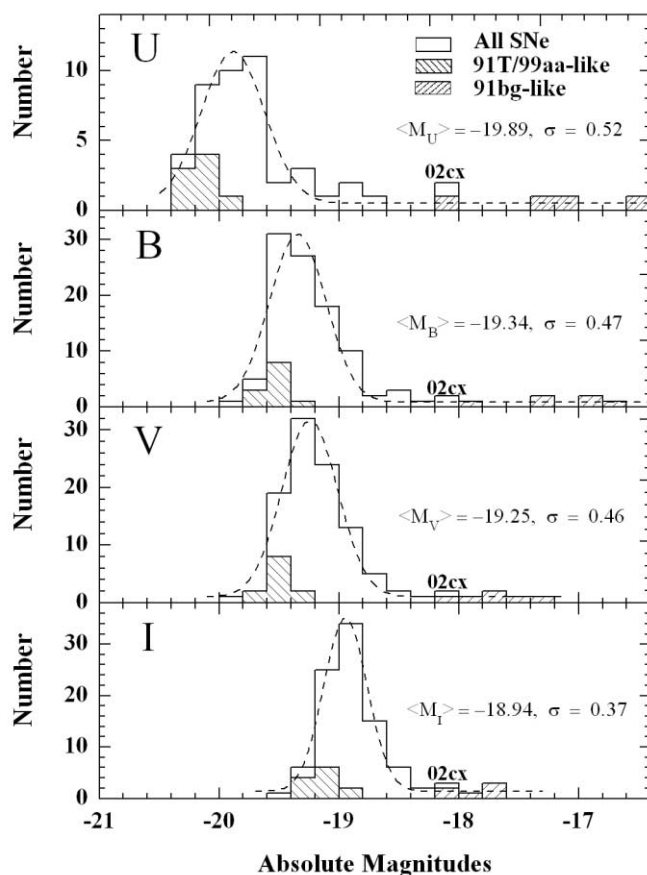


FIG. 5.—Distribution of the absolute magnitudes at maximum for 109 SNe Ia in $UBVI$ bands. The Gaussian fit (dashed lines) to the absolute magnitudes, the mean values, and the standard deviations are also shown.

The spectroscopically peculiar, SN 1991T-like and SN 1999aa-like events lie at the brighter end of the luminosity distribution of SNe Ia, which are ~ 0.3 mag brighter than the normal ones. Moreover, these overluminous events seem to have relatively uniform peak luminosity, with a small scatter of about 0.13 mag in the BVI and 0.20 mag in the U band. On the other hand, the faintest SNe Ia are almost characterized by the SN 1991bg-like events but for the most peculiar SN 2002cx. In contrast to the SN 1991T/SN 1999aa-like SNe Ia, the SN 1991bg-like events cover a wider range of peak luminosities from ~ 2 to ~ 0.6 mag in different wave bands. The luminosity distributions of SNe Ia in $UBVI$ bands can be roughly fitted by Gaussians. The long tail at the faint end indicates a continuous distribution of the peak luminosities between the Branch normal SNe Ia (Branch et al. 1993) and the SN 1991bg-like events, possibly suggesting a common origin for their progenitors.

4.2. The Environmental Effects on SN Ia Luminosity

Locations of the SNe in their host galaxies may offer clues to understand the origin of SN Ia optical diversities (Wang et al. 1997), as the properties of the stellar populations (e.g., metallicity and age) may vary from galaxy to galaxy and vary with the spatial positions within a galaxy. In Figure 6 we show the radial distribution of the absolute magnitudes M_B corrected for the absorption in the Galaxy and the host galaxy as laid out in § 3. The SN location (here we only considered the radial position) is defined as the relative galactocentric distance r_{SN}/r_{25} , where r_{SN} is the deprojected radial distance of the SNe Ia from the galactic

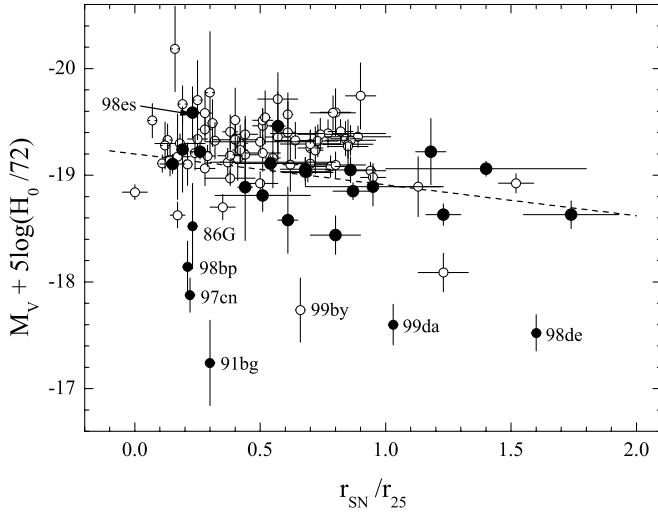


FIG. 6.—Absolute magnitudes M_V (fully corrected for the extinction) plotted against the relative radial distance r_{SN}/r_{25} . The open circles show the spiral galaxies, and the filled circles represent the E/S0 galaxies. The larger filled circles are for the normal SNe Ia in E/S0 galaxies.

center and r_{25} is the de Vaucouleurs radius of that galaxy (e.g., de Vaucouleurs et al. 1991).

To examine the age effect on SN Ia luminosity, we treat SNe in late types (spiral galaxies) and early types (S0 and elliptical galaxies) separately, where the stellar populations are assumed to be different. We find that SN Ia luminosity is related to the morphological types of the host galaxies. Brighter SNe Ia tend to occur in spiral galaxies with younger stellar populations, while most of the fainter events occur preferentially in the E/S0 galaxies with relatively older stars. This dichotomy was first noticed by Hamuy et al. (1996a) and later confirmed by Riess et al. (1999) and Hamuy et al. (2000). This observational fact argues for the age difference in the progenitors as the origin of SN Ia optical diversities. Nevertheless, such an age effect alone seems unlikely to account for the occurrence of the brighter object SN 1998es (with $\Delta m_{15} = 0.87$) in the lenticular galaxy NGC 632 and the presence of the fainter event SN 1999by (with $\Delta m_{15} = 1.90$) in the Sb galaxy NGC 2841.

On the other hand, we did not find any radial variation for SN Ia luminosity in spiral galaxies alone, which is consistent with previous studies (Parodi et al. 2000; Ivanov et al. 2000). The SNe in E/S0 galaxies (*filled circles*) at first glance do not show any significant correlation between the luminosity and the SN spacial position r_{SN}/r_{25} . Omitting arbitrarily those peculiar SNe Ia, e.g., the SN 1991bg-like events as labeled in Figure 5, however, a trend with the galactocentric distances seems to emerge for the others. A radial gradient of 0.30 ± 0.12 was found for normal SNe Ia in E/S0 galaxies, which is significant at a confidence level of $\sim 2.5 \sigma$.

If the magnitude gradient observed for normal SNe Ia in E/S0 galaxies was true, then the radial metallicity variation in elliptical galaxies (Henry & Worthey 1999) may be responsible for the diversities of SN Ia luminosities because the stellar populations in these earlier galaxies are generally believed to be coeval (Worthey 1994; Vazdekis et al. 1997). Theoretically, the metallicity effect on the range of SN Ia luminosity may be understood by the “strong wind” models proposed by Umeda et al. (1999), who suggest that the lower metallicity systems will tend to have larger initial C/O masses and hence fainter SNe Ia. The lack of magnitude gradient in spiral galaxies may be the counteracting result from the effects of both age and metallicity because the stellar populations in the inner regions of spiral galaxies are, however, in general more metal-rich and older in relation to those in the outer regions (Henry & Worthey 1999). In order to further disentangle these two environmental aspects, one may need to resort to the spectroscopic studies of SN Ia host galaxies as suggested by Hamuy et al. (2000).

4.3. Luminosity Dependence of SNe Ia on the Secondary Parameters

The correlations between SN Ia peak luminosities and the secondary parameters were specifically investigated by Parodi et al. (2000) and have recently been revisited by R05. Their studies suggested that the decline rate Δm_{15} and the peak $B - V$ color (see also Tripp 1997; Tripp & Branch 1999) are the two key parameters for the homogenization of SN Ia luminosities. To examine this relationship, the absorption-corrected absolute magnitudes M_V of 73 Hubble flow SNe (see the definition in § 5.1) are thus plotted against the decline rate Δm_{15} , the peak $B - V$ color, and the postmaximum color ΔC_{12} in Figure 7. The 11 nearby SNe Ia with

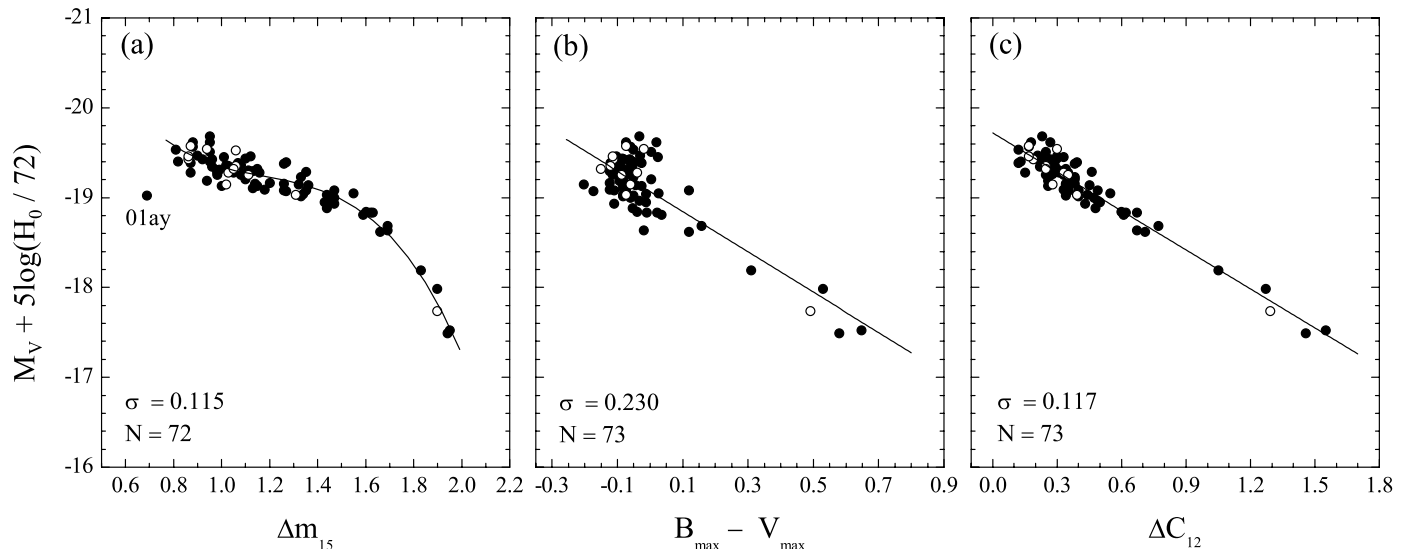


FIG. 7.—Absolute magnitudes M_V , fully corrected for extinction, vs. the decline rate Δm_{15} , the peak color $B - V$, and the postmaximum color ΔC_{12} . Filled circles show the Hubble flow SN sample, and the open circles represent the nearby calibrators.

TABLE 3
COEFFICIENTS OF THE RELATIONS BETWEEN PEAK LUMINOSITY, COLOR PARAMETER ΔC_{12} , AND THE HOST GALAXY REDDENING

Bandpass	N^a	b	R	M^0	σ_M
U	29	2.65(10)	4.37(25)	-19.87(05)	0.162
B	73	1.94(06)	3.33(11)	-19.34(02)	0.120
V	73	1.44(06)	2.30(11)	-19.27(02)	0.117
I	69	1.00(05)	1.18(11)	-18.96(02)	0.112

^a N is the number of Hubble flow SNe Ia used to determine the relation.

Cepheid distance calibrations from Table 5 are also overlaid in the figure.

The dependence of SN Ia peak luminosity on the decline rate Δm_{15} becomes apparently nonlinear for the full SN sample with different spectral types as shown in Figure 7a. Excluding SN 2001ay, however, a cubic spline seems to give a perfect fit to the M_V - Δm_{15} relation with a dispersion of ~ 0.12 mag. The cubic polynomial dependence and the small dispersion are expected if the color term ΔC_{12} in equation (4) is substituted by the right-hand side of equation (1).

Figure 7b shows the M_V - $(B_{\max} - V_{\max})$ plot. Although the peak color $B_{\max} - V_{\max}$ connects well with fainter SNe Ia at the redder end, it is very loosely related to the peak luminosity for most of the SNe Ia with $-0.1 \text{ mag} \lesssim B_{\max} - V_{\max} \lesssim 0.1 \text{ mag}$. The linear fit yields a larger dispersion of ~ 0.23 mag for the points in Figure 7b, which indicates that the peak color alone cannot delineate the peak luminosity of SNe Ia. Combining both Δm_{15} and $B_{\max} - V_{\max}$ in the homogenization can reduce the luminosity dispersion to ~ 0.16 mag, which is consistent with that obtained by R05.

The correlation of the extinction-corrected absolute magnitudes with ΔC_{12} is illustrated in Figure 7c. As it can be seen, the tight and linear M_V - ΔC_{12} relation found for the reddening-free SNe still holds well for the larger SN sample. The rms scatter yield along the best-fit line is $\lesssim 0.12$ mag in BVI , which corresponds to a distance uncertainty of 5%–6%. As the host galaxy reddening $E(B - V)_{\text{host}}$ was also partially derived from the observed color ΔC_{12} , it is necessary to examine the possible inter-

play of these two variables. The corresponding regression with these two variables takes the form of

$$M_{UBVI} = b_{UBVI} [\Delta C_{12} - E(B - V)_{\text{host}} - 0.31] + R_{UBVI} E(B - V)_{\text{host}} + M_{UBVI}^0, \quad (7)$$

leading further to

$$M_{UBVI} = b_{UBVI} (\Delta C_{12} - 0.31) + (R_{UBVI} - b_{UBVI}) E(B - V)_{\text{host}} + M_{UBVI}^0, \quad (8)$$

where the constant term, M_{UBVI}^0 , is the mean absolute magnitude reduced to $\Delta C_{12} = 0.31$. Least-squares solutions for all 73 Hubble flow SNe in Figure 7 give the values of b_{UBVI} , R_{UBVI} , and M_{UBVI}^0 as shown in Table 3. The improved R_{UBVI} values are very close to the provisional values determined from Figure 4, and the slopes of the correlation b_{UBVI} agree quite well with those shown in equations (2)–(5). This suggests that the two variables $E(B - V)_{\text{host}}$ and ΔC_{12} are quite independent of each other. Note that the slope of the correlation and the reddening ratio show very similar values in the I band. In other words, we can homogenize well the I -band luminosity of SNe Ia by the single parameter ΔC_{12} without knowing the host galaxy reddening (because the second term on the right-hand side of eq. [8] approximately drops out).

The small dispersion given by the M - ΔC_{12} relation (see Table 3 and Fig. 7) leaves little room for the dependence of SN Ia luminosity on other secondary parameters. To further strengthen our case, we examine the remaining dependence of the M_V - ΔC_{12} relation fits on other secondary parameters (see Fig. 8). After homogenization as to ΔC_{12} according to equation (7), the magnitude residuals δM_V from the best fit in Figure 7c did not show any significant dependence on the decline rate Δm_{15} , or on the peak $B - V$ color. As can be seen from Figure 8, the luminosity gradient with the galactocentric distances r_{SN}/r_{25} found for SNe Ia in E/S0 galaxies also becomes marginally important with a confidence level of $\lesssim 1 \sigma$. This shows that the environmental effects (such as the metallicity and/or the age of the progenitors) on SN peak luminosity can be removed or substantially reduced via ΔC_{12} calibration.

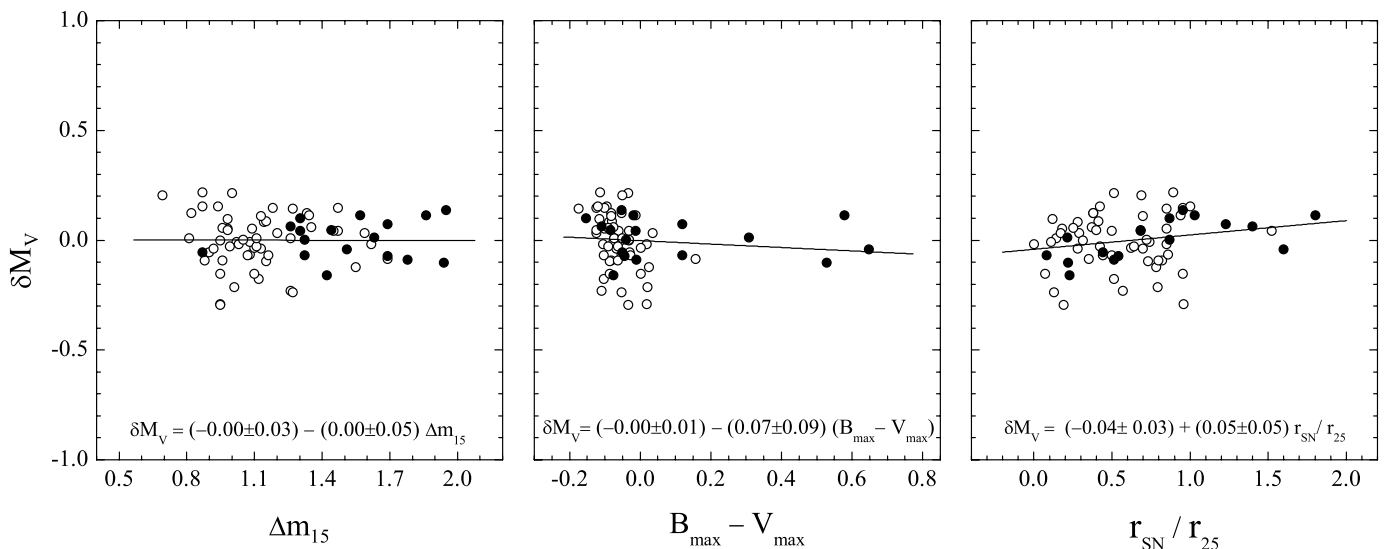


FIG. 8.—Residuals of the M_V - ΔC_{12} relation fits for M_V plotted against the decline rate Δm_{15} , the peak color $B_{\max} - V_{\max}$, and the location of the SNe Ia in their host galaxies. The open circles are for spiral galaxies, and the filled circles are for E/S0 galaxies.

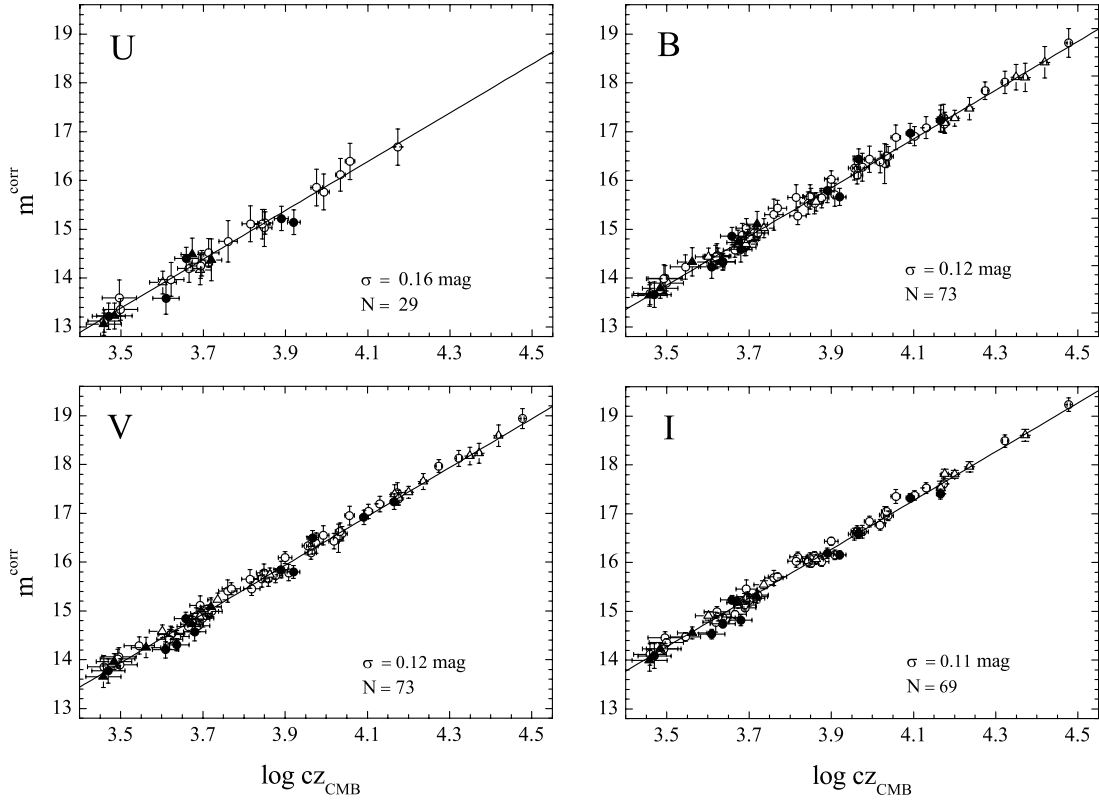


FIG. 9.—Hubble diagrams in U , B , V , and I for 73 SNe Ia with $0.01 \lesssim z \lesssim 0.1$, which were calibrated using ΔC_{12} . SNe Ia in spiral galaxies are shown with circles, while those in E/S0 galaxies are shown with triangles. The open symbols are for normal SNe Ia, and the filled symbols are for the spectroscopically peculiar events. The best-fit linear regressions are shown, with a dispersion of ~ 0.16 mag in the U band and $\lesssim 0.12$ mag in the BVI bands.

The M - ΔC_{12} relation is reexamined and confirmed for a larger SN sample, which allows us to calibrate SNe Ia using ΔC_{12} with more confidence. It should be emphasized that this is still not a universal relation, as there are still extremely “anomalous” or rare events, such as SN 2002cx, which cannot be calibrated by any known methods.

5. THE DISTANCE SCALES

5.1. The Hubble Diagram of SNe Ia

An effective way of assessing the quality of SNe Ia as distance indicators is to plot them in the Hubble diagram. The two quantities entering the Hubble diagram, magnitude m and redshift z , are direct tracers for the expansion history of the universe. Our data sample consists of 109 well-observed SNe Ia; nevertheless, not all of them are suitable for constructing the Hubble diagram and exploring the expansion rate of the universe. We have intentionally excluded those SNe Ia in galaxies with $cz \lesssim 3000$ km s $^{-1}$ to reduce the uncertainties from the peculiar motions. In addition, we further excluded SN 1996ab with $cz = 37,370$ km s $^{-1}$, where the cosmological effect on the luminosity distance becomes important (Jha et al. 1999). After these selections, the remaining sample consists of 73 SNe Ia in the Hubble flow.

At distances of $z \lesssim 0.1$, the dimming of a standard candle as a function of redshift z can be simply described by

$$m = 5 \log cz + \alpha, \quad (9)$$

where cz is the recession velocity corrected to the CMB frame and α is the “intercept of the ridge line” given by

$$\alpha = M + 25 - 5 \log H_0. \quad (10)$$

It follows immediately that

$$H_0 = 10^{0.2(M+25-\alpha)}. \quad (11)$$

By equation (11), determination of the Hubble constant H_0 from SNe requires their absolute magnitudes and the intercept of their Hubble lines. The absolute magnitudes are obtained by observations of nearby SNe Ia with Cepheid distances (see § 5.2), while the intercept α can be determined by observations of the Hubble flow ones.

In Figure 9 we present the U -, B -, V -, and I -band Hubble diagrams (or m - z relation) for the 73 Hubble flow SNe Ia. The apparent magnitudes are corrected for the ΔC_{12} dependence and the host galaxy absorption according to equation (7). The small scatter in the Hubble diagram allows us to solve precisely for the α -value in equation (9), which is -4.18 ± 0.03 in U , -3.64 ± 0.01 in B , -3.56 ± 0.01 in V , and -3.25 ± 0.01 in I . To test the robustness of the global fit, we examined the m - z relation using different subsets of the SN sample in the Hubble flow. This includes the recession velocity, the host galaxy reddening, and the spectral types of SNe Ia. The best-fit results are summarized in Table 4. Note that the number shown in column (2) of Table 2 refers to the SN number with available data in the B and V bands.

The Hubble lines defined by SNe Ia with different spectral types (e.g., normal, SN 1991T/SN 1999aa-like, and SN 1991bg-like) may have remarkable offsets in the zero points, due to the larger difference between their intrinsic luminosities (see Fig. 5). As a test of the spectral dependence, we examined the Hubble diagrams constructed by normal, SN 1991T/SN 1999aa-like, and SN 1991bg-like SNe Ia, respectively. It turns out that the α -values derived from the peculiar SNe Ia are consistent with the global fit

TABLE 4
BEST-FITTING RESULTS OF THE m - z RELATION FOR DIFFERENT SN Ia SAMPLES

Sample	N_{BV} ^a	α_U	σ_U	α_B	σ_B	α_V	σ_V	α_I	σ_I
All	73	-4.18(03)	0.162	-3.64(01)	0.120	-3.56(01)	0.117	-3.25(01)	0.112
Normal	58	-4.14(03)	0.113	-3.63(01)	0.104	-3.54(01)	0.099	-3.23(02)	0.091
Normal, $v < 7000$	26	-4.17(05)	0.113	-3.65(03)	0.118	-3.56(02)	0.108	-3.24(02)	0.102
Normal, $v > 7000$	32	-4.06(06)	0.104	-3.63(02)	0.093	-3.53(03)	0.091	-3.21(02)	0.081
Normal, $E(B - V)_{\text{host}} \leq 0.15$	47	-4.14(04)	0.126	-3.63(02)	0.090	-3.53(02)	0.087	-3.22(02)	0.087
Normal, $E(B - V)_{\text{host}} \leq 0.06$	24	-4.18(07)	0.177	-3.64(02)	0.078	-3.55(02)	0.074	-3.25(02)	0.071
SN 1991T/SN 1999aa-like	10	-4.28(08)	0.206	-3.70(06)	0.175	-3.69(04)	0.138	-3.35(05)	0.161
SN 1991bg-like	4	-4.14(15)	0.228	-3.55(08)	0.083	-3.56(07)	0.093	-3.26(07)	0.082

^a N_{BV} represents the number of SNe Ia available in the B and V bands.

within ± 0.15 mag (see Table 4). Including a fraction of $\sim 20\%$ peculiar events in the full SN sample appears not to affect the Hubble line. This is demonstrated by the statistically insignificant variations in the α -values between the full sample and the sample of 58 normal ones.

As the normal SNe Ia look more uniform, with a small scatter of about 0.10 mag in $UBVI$ bands, they are appropriately used to probe the possible variation in the expansion rate. Zehavi et al. (1998) suggested a dynamic glitch in the Hubble diagram of SNe Ia at $cz = 7000$ km s⁻¹, across which the expansion rate of the local universe may change by a few percent. To examine this effect and the possible variation in α , we divided the sample of 58 normal SNe Ia into two subsamples using the velocity cut at 7000 km s⁻¹. The variations of the α -values between the more distant SNe Ia and the nearby ones are found to be around 0.03 mag in BVI bands, which would lead to a discrepancy in the expansion rate of less than 2%. The larger difference shown in the U band is more likely due to a statistical fluke since there are only seven SNe Ia with U -band photometry beyond $v = 7000$ km s⁻¹. However, more Hubble flow SN Ia samples and various analysis techniques are still needed to further diagnose the discontinuity of the expansion rate at the local universe.

To explore the effect of the absorption corrections on the Hubble line, we considered the cases with restrictions on the maximum value of $E(B - V)_{\text{host}}$ in the fitting. Excluding the highly reddened SNe [i.e., $E(B - V)_{\text{host}} > 0.15$ mag], or even the SNe with $E(B - V)_{\text{host}} > 0.06$ mag from the Hubble diagram, the change in the α -value is ≤ 0.02 mag in each wave band. This argues in favor of the self-consistent determinations of the host galaxy reddening and the unconventional R_{UBVI} values. Assuming the scatters shown by the fit to SNe Ia with minimum absorption [e.g., $E(B - V)_{\text{host}} \leq 0.06$ mag] as the intrinsic ones, we can estimate the uncertainties caused by the absorption corrections. By comparing them with those values shown in the fit of all normal SNe Ia, we place a limit on the errors of the absorption corrections of ~ 0.08 , 0.07, and 0.06 mag in the B , V , and I bands, respectively. This is slightly smaller than the corresponding value derived from the error of the host galaxy reddening given in Table 1. The small number of statistic samples prevented us from giving a reasonable value in the U band.

It is satisfactory that the Hubble flow SNe Ia of different subsets yield the same α -values in each wave band within the errors, showing the robustness of the ΔC_{12} method. In particular, the dispersion around the Hubble line is impressively small for each subset of the SN sample. For example, the dispersion for the sample of 58 normal SNe Ia is only 0.09–0.10 mag in full optical bands, corresponding to a $\sim 5\%$ relative distance uncertainty

per SN.⁷ For comparison, the MLCS method yields $\sigma_B = 0.22$ mag for their gold sample of 67 SNe Ia (Riess et al. 2004), whereas the BATM calibration yields $\sigma_B = 0.21$ mag (BATM; Tonry et al. 2003). The two-parameter method (which involves both Δm_{15} and peak $B - V$ color corrections) revisited recently by R05 gives a dispersion of 0.16 mag for 63 SNe Ia. In an approximately parallel analysis, Wang et al. (2006) obtained an rms scatter of $\sigma_B \approx 0.14$ mag for 33 selected SNe Ia. The SALT method (Guy et al. 2005) gives $\sigma_B = 0.16$ mag for a sample of 23 SNe Ia. In reference to the above calibration methods, the ΔC_{12} method improves remarkably the distance accuracy from SNe Ia. This will invoke hopefully more precise determinations of the Hubble constant H_0 and other cosmological parameters. The application of the ΔC_{12} method to the Supernova Legacy Survey data (Astier et al. 2006) will be presented in a forthcoming paper.

5.2. Calibrations of the Absolute Magnitudes of SNe Ia

In order to infer the Hubble constant H_0 , it is necessary to tie our ΔC_{12} distances to the SNe Ia with absolute magnitude calibrations. Cepheid variables, currently, through their period-luminosity (P - L) relation, are the fundamental primary distance indicators. We can thus establish the absolute magnitudes of SNe Ia through the distances measured from the Cepheid variables in their host galaxies.

Thanks primarily to the valuable contribution of the Saha-Tammann-Sandage SN Ia *Hubble Space Telescope* (*HST*) Calibration Project (hereafter STS), the number of SNe Ia with Cepheid distances to their host galaxies has increased to 13 so far. The STS consortium provided the Cepheid distances to SN 1895B (NGC 5253), SN 1937C (IC 4182), SN 1972E (NGC 5253), SN 1981B (NGC 4536), SN 1960F (NGC 4496A), SN 1990N (NGC 4639), SN 1989B (NGC 3627), SN 1998aq (NGC 3982), and SN 1991T (NGC 4527; Saha et al. 1996, 1997, 1999, 2001a, 2001b). The Cepheid distances to SN 1974G in NGC 4414, SN 1998bu in NGC 3368, and SN 1999by in NGC 2841 were obtained by Turner et al. (1998), Tanvir et al. (1999), and Macri et al. (2001), respectively. Using the Advanced Camera for Surveys (ACS) on *HST*, Riess et al. (2005) recently measured the Cepheid distance to the more distant SN 1994ae in NGC 3370. These SNe Ia with Cepheid distances will provide the calibration for the absolute magnitudes of SNe Ia.

Nevertheless, analysis of the preceding Cepheid data does not reach a consistent result on the absolute calibration for SN Ia

⁷ Considering the typical uncertainties of the redshift due to peculiar velocity (e.g., 300 km s⁻¹ adopted in our analysis), the actual uncertainty intrinsic to our ΔC_{12} distance calibration is less than 4%, which can be fully interpreted as the photometric errors.

peak luminosity (see also discussions by Riess et al. 2005). Compared with the results of STS, the distances reanalyzed by the *HST* key project (hereafter KP) are on average shorter by 0.2–0.3 mag (Gibson et al. 2000; Freedman et al. 2001). This discrepancy may arise primarily from the sample selection of the Cepheid variables and the choice of the P - L relation (i.e., Saha et al. 2001b). The STS consortium used the earlier P - L relation that was established by Madore & Freedman (1991), while the KP group employed a new P - L relation that is based on the Cepheid data of the Optical Gravitational Lensing Experiment (OGLE) survey (Udalski et al. 1999). The OGLE P - L relation, with a flatter color-period relation of $(V - I) \propto 0.2 \log P$, yields a shorter Cepheid distance by about 8% than that derived from the earlier Madore & Freedman (1991) relation. We preferred the OGLE-based P - L relation and the resulting Cepheid distances (i.e., the KP distances; Freedman et al. 2001) in this paper, due to the well-sampled light curves and the accurate photometry of the OGLE Cepheids (Udalski et al. 1999; Sebo et al. 2002).

The Cepheid P - L relation derived from the LMC was traditionally considered to be universal for all other galaxies. However, there is increasing evidence for a significant dependence of the Cepheid properties on the metallicity of the host stellar populations. An empirical test of this dependence by Kennicutt et al. (1998) yielded $\Delta\mu_0/\Delta[\text{O}/\text{H}] = -0.24 \pm 0.16 \text{ mag dex}^{-1}$. Such a dependence is in agreement with the theoretical predictions by Fiorentino et al. (2002). Using a larger sample of 17 Cepheid hosts with independent distances, Sakai et al. (2004) obtained a more robust empirical correction relation $\Delta\mu_0/\Delta[\text{O}/\text{H}] = -0.24 \pm 0.05 \text{ mag dex}^{-1}$ with reduced errors, which is adopted here as metallicity correction for Cepheid distances.

Table 5 contains a list of partial parameters for 11 nearby SNe Ia with Cepheid distances (see Table 1 for other parameters in more detail). The two historical SNe SN 1895 and SN 1960F were not included because their V light curves are unavailable to infer the ΔC_{12} value and hence the host galaxy reddening. The KP distance moduli of these calibrators, with and without the metallicity corrections, are given in columns (3) and (4). The apparent V magnitudes (corrected for the Galactic absorption), the color parameter ΔC_{12} , and the host galaxy reddening are listed in columns (5)–(7). The fiducial magnitudes m_V^0 , corrected for absorption and ΔC_{12} using equation (8), are given in column (8). The final absolute magnitudes of the calibrators, M_U^0 , M_B^0 , M_V^0 , and M_I^0 contained in columns (9)–(12), respectively, are derived by subtracting the distance moduli $\mu_{\text{KP}}(Z)$ from the corresponding apparent magnitudes m_{UBVI}^0 (here we only listed in Table 5 the case for apparent V magnitudes for the space limit). The uncertainties associated with the absolute magnitudes for each calibrator were obtained by combining in quadrature the quoted errors δm , $\delta\Delta C_{12}$, $\delta E(B - V)_{\text{host}}$, and $\delta\mu_{\text{KP}}(Z)$.

The weighted averages of the peak absolute magnitudes in $UBVI$ for the 11 nearby calibrators, reduced to $\Delta C_{12} = 0.31$ using equation (8) and the coefficients listed in Table 3, are given as

$$M_U = -19.89 \pm 0.08 \text{ mag}, \quad \sigma_U = 0.14 \text{ mag}, \quad (12)$$

$$M_B = -19.33 \pm 0.06 \text{ mag}, \quad \sigma_B = 0.11 \text{ mag}, \quad (13)$$

$$M_V = -19.27 \pm 0.05 \text{ mag}, \quad \sigma_V = 0.11 \text{ mag}, \quad (14)$$

$$M_I = -18.97 \pm 0.04 \text{ mag}, \quad \sigma_I = 0.08 \text{ mag}. \quad (15)$$

Excluding the spectroscopically peculiar SN 1991T and SN 1999by, or further dropping the highly reddened SN 1989B and SN 1998bu from the analysis, the change in the mean value of

the absolute magnitudes at maximum is minor (i.e., $\lesssim 0.03 \text{ mag}$). If the metallicity effect was not taken into account, the distances to SN Ia host galaxies and consequently the peak luminosity of SNe Ia would be underestimated by $\sim 0.1 \text{ mag}$. Meanwhile, the scatter of the mean absolute magnitudes would increase significantly, i.e., from ~ 0.11 to 0.16 mag in the V band. This also argues in favor of the metallicity correction of the Cepheid distances purely by virtue of reducing the luminosity dispersion of the SN calibrators.

Inspection of the M^0 values listed in Table 3 shows that the Hubble flow SNe Ia have approximately the same absolute magnitudes as the more nearby ones calibrated via Cepheids. This fact suggests that the value of H_0 ($72 \text{ km s}^{-1} \text{ Mpc}^{-1}$), assumed for determining the distances to the SNe in the Hubble flow, must have been very close to the H_0 value implied from the KP Cepheid distances. This similarity is not a foregone conclusion but results from a coincidence. If we take the distance moduli from STS to calibrate SNe Ia, however, the predicted absolute magnitudes of SNe Ia would increase by $\sim 0.25 \text{ mag}$, i.e., $M_B = -19.58 \pm 0.06 \text{ mag}$ and $M_V = -19.51 \pm 0.05 \text{ mag}$, which will lead to a Hubble constant of $\sim 65 \text{ km s}^{-1} \text{ Mpc}^{-1}$, lower than the assumed value.

Combinations of the peak absolute magnitudes M_{UBVI}^{corr} shown in equations (12)–(15) with the individual apparent magnitudes m_{UBVI}^{corr} of 109 SNe Ia can give the luminosity distances to 109 SNe Ia (Table 2, cols. [6]–[9]). The luminosity distances, especially those in the U band, are important for comparison between the cosmological distances of SNe Ia beyond $z \geq 0.8$. The distance moduli presented in Table 2 can also be used to constrain the peculiar motions of the nearby galaxies hosting SNe Ia.

5.3. Determination of the Hubble Constant H_0

Taking the zero points of the Hubble lines from Table 4 and inserting the absolute magnitudes of the SN calibrators into equation (11), we can obtain the value for the Hubble constant H_0 . The key results for five different combinations of the Hubble flow SNe Ia and the nearby calibrators are summarized in Table 6.

For all of the Hubble flow SNe ($N = 73$) and the nearby calibrators ($N = 11$), the combination yields consistent determinations of $H_0 = 72 \pm 2$ in the B , V , and I bands; the smaller value yielded in the U band may be due to the statistical fluctuation. Omitting 14 peculiar SNe from the Hubble flow and two from the nearby calibrators, the similar procedure reproduced well the $H_0(U, B, V, I)$ values for the full sample. By further eliminating the highly reddened SNe [i.e., those with $E(B - V)_{\text{host}} > 0.15 \text{ mag}$], one finds similar $H_0(U, B, V, I)$ values from the remaining sample ($47 + 7$). We also examined the extreme case for the spectroscopically peculiar SNe Ia. For SN 1991T/SN 1999aa-like SNe Ia, the resulting H_0 value is 68 ± 3 , while the SN 1991bg-like events give a value of 75 ± 5 . It is reassuring that both the normal SNe Ia and the peculiar ones yield consistent determinations of the Hubble constant within the errors.

In all of the above five cases, the weighted mean value of H_0 is within $68 \leq H_0 \leq 75$. This suggests that our results are not sensitive to different subsets of SNe Ia, and that no obvious systematic errors are being introduced by absorption corrections or including the peculiar SNe in the analysis. Taking the former three cases shown in Table 6 as the most consistent determinations, a value of 72 ± 1 is obtained for the Hubble constant. Restricting the analysis to the four best calibrators of SN 1981B, SN 1990N, SN 1994ae, and SN 1998aq as ranked by Riess et al. (2005), the resulting H_0 value remains almost unchanged. Taking into account the intrinsic luminosity dispersion implied from

TABLE 5
ABSOLUTE MAGNITUDES OF SNe Ia WITH CEPHEID DISTANCES

SN (1)	Galaxy (2)	μ_{KP} (3)	$\mu_{KP}(Z)$ (4)	m_V (5)	ΔC_{12} (6)	$E(B - V)_{\text{host}}$ (7)	m_V^0 (8)	M_U^0 (9)	M_B^0 (10)	M_V^0 (11)	M_I^0 (12)
1937C.....	IC 4182	28.28(06)	28.26(06)	8.77	0.21	0.04	8.89(13)	...	-19.38(18)	-19.38(16)	...
1972E.....	NGC 5253	27.56(14)	27.48(14)	8.17	0.24	0.05	8.24(12)	-19.94(30)	-19.30(22)	-19.25(19)	...
1974G.....	NGC 4414	31.10(05)	31.27(06)	12.34	0.47	0.15	11.99(22)	...	-19.34(29)	-19.29(26)	...
1981B.....	NGC 4536	30.80(04)	30.88(04)	11.92	0.47	0.12	11.59(08)	-19.79(28)	-19.40(21)	-19.29(16)	...
1989B.....	NGC 3627	29.86(08)	30.04(09)	11.88	0.76	0.37	10.93(10)	-19.96(29)	-19.41(23)	-19.26(18)	-18.98(13)
1990N.....	NGC 4639	31.61(08)	31.73(08)	12.64	0.36	0.11	12.48(08)	-19.81(21)	-19.34(17)	-19.25(14)	-18.91(11)
1991T.....	NGC 4527	30.48(09)	30.58(09)	11.44	0.48	0.18	11.05(09)	-20.18(21)	-19.56(18)	-19.54(15)	-19.15(12)
1994ae.....	NGC 3370	32.22(06)	32.29(06)	12.94	0.22	0.05	13.04(08)	-19.80(21)	-19.25(16)	-19.23(13)	-18.95(09)
1998aq.....	NGC 3982	31.60(09)	31.66(09)	12.41	0.28	0.03	12.43(07)	-19.98(20)	-19.35(17)	-19.23(13)	-18.95(11)
1998bu.....	NGC 3368	29.97(06)	30.14(07)	11.80	0.64	0.36	11.03(09)	-19.86(20)	-19.17(16)	-19.12(13)	-18.94(11)
1999by.....	NGC 2841	30.74(23)	30.84(23)	13.10	1.29	0.00	11.66(11)	-19.71(30)	-19.15(27)	-19.15(25)	-18.95(25)
Mean	-19.89(08)	-19.33(06)	-19.27(05)	-18.97(04)
Mean (excluding SN 1991T and SN 1999by).....	-19.87(09)	-19.32(06)	-19.24(05)	-18.95(05)
Mean (excluding SN 1989B and SN 1998bu).....	-19.86(10)	-19.34(07)	-19.27(07)	-18.94(06)

TABLE 6
 VALUE OF THE HUBBLE CONSTANT H_0 (IN $\text{km s}^{-1} \text{Mpc}^{-1}$) FROM SNe Ia

Sample ($N_h + N_c$) ^a	$H_0(U)$	$H_0(B)$	$H_0(V)$	$H_0(I)$	$H_0(U, B, V, I)$
All (73+11)	72.1±2.9	72.8±2.1	72.1±1.8	71.8±1.4	72.1±0.9
Normal (58+9)	71.4±3.5	72.8±2.1	72.4±2.1	71.8±1.8	72.2±1.1
Normal, $E(B - V)_{\text{host}} \leq 0.15$ (47+7)	71.8±3.6	72.1±2.5	71.1±2.3	71.8±2.1	71.7±1.2
SN 1991T/SN 1999aa-like (10+1)	66.1±6.9	67.3±5.9	67.6±4.9	69.2±4.2	67.9±2.6
SN 1991bg-like (4+1)	76.9±12.0	75.9±9.9	76.2±9.8	72.8±8.7	75.1±5.0

^a N_h is the number of SNe in the Hubble flow sample, while N_c is the number of nearby calibrators.

the Hubble flow SNe Ia, e.g., $\lesssim 0.12$ mag in BVI bands, the H_0 value becomes

$$H_0 = 72 \pm 4 \text{ (statistical) km s}^{-1} \text{Mpc}^{-1}. \quad (16)$$

The uncertainty accounts for the statistical error of the absolute magnitude calibration of nearby calibrators and the dispersion in the Hubble diagram of Hubble flow SNe Ia.

In accord with Riess et al. (2005), especially their Table 13 (but also see Freedman et al. [2001] for more detailed discussions of the systematic error budget), two main sources of error were incorporated into the systematic error budget. Uncertainties in the LMC zero point enter at a level of 0.10 mag, and the slope of the P - L relation is at a level of 0.05 mag. In quadrature, the overall systematic error budget amounts to 0.11 mag, corresponding to about 6% in H_0 . In combination with the statistical error and the systematic error, the final result for the Hubble constant yields

$$H_0 = 72 \pm 4 \text{ (statistical)} \pm 4 \text{ (systematic)} \\ = 72 \pm 6 \text{ (total) km s}^{-1} \text{Mpc}^{-1}. \quad (17)$$

This H_0 value, based on the homogenization of the ΔC_{12} method, is in excellent agreement with that determined by the MLCS2k2 method (Riess et al. 2005) and is also fully consistent with the determinations from the *Wilkinson Microwave Anisotropy Probe* (WMAP) data (Spergel et al. 2003). However, the true uncertainty in our value of the Hubble constant may indeed be somewhat larger than our formal value due to the controversial Cepheid distances to the SN Ia host galaxies (e.g., Saha et al. 2006; Sandage et al. 2006).

6. DISCUSSION AND CONCLUSIONS

A larger sample of 109 SNe Ia has been compiled from the literature to investigate the properties of the dust in their host galaxies. Using the host galaxy reddening derived from ΔC_{12} and the tail colors of SNe Ia, we found smaller values for the reddening ratios of $R_U = 4.37 \pm 0.25$, $R_B = 3.33 \pm 0.11$, $R_V = 2.30 \pm 0.11$, and $R_I = 1.18 \pm 0.11$, which are smaller than the standard R_{UBVI} values of 5.5, 4.3, 3.3, and 1.8, respectively. The drastic explosion of the SNe may in some manner change the distribution of the dust grains surrounding the SN. Another possible explanation for the observed lower values of R turns to the dust in the circumstellar environment of SNe (Wang 2005), which may be substantially different from the interstellar dust.

In particular, we have discussed the luminosity dependence on the environmental parameters, such as the morphological type of the host galaxy and the location of the SNe within the galaxy. As first noted by Hamuy et al. (2000) and confirmed by our study, the brighter SNe prefer to occur in the late-type (spiral) galaxies and the fainter ones prefer to occur in the early-type (E/S0) galaxies. However, there are two counterexamples: one is SN

1998es, which was an SN 1991T-like event and exploded in the lenticular galaxy NGC 632; the other is SN 1999by, which was an SN 1991bg-like event and occurred in the Sb-type galaxy NGC 2841. These two cases suggest that the age may not be an exclusive factor underlying SN Ia diversities. The radial gradient of the absolute magnitudes (at a confidence of $\sim 2.5 \sigma$) found for normal SNe Ia in E/S0 galaxies implies that the metallicity is probably another important factor responsible for the range of SN Ia luminosities.

Using 73 Hubble flow SNe Ia, we also examined the correlations between SN Ia luminosities and the secondary parameters such as the decline rate Δm_{15} , the peak $B - V$ color, and the postmaximum color ΔC_{12} . We found that the relation between the peak luminosity and the light-curve shapes becomes apparently nonlinear, and a more complicated function is needed to describe this relationship. The correlation of the peak luminosity and the peak color shows a large scatter of ~ 0.23 mag around the best-fit line, which is not tight enough to get reliable calibrations for SNe Ia. Compared with Δm_{15} and $B_{\text{max}} - V_{\text{max}}$, the color parameter ΔC_{12} can depict extremely well the peak luminosity of SNe Ia, with an impressively small dispersion of $\lesssim 0.12$ mag in BVI . One example to illustrate the superiority of ΔC_{12} calibration is SN 2001ay, which has a very broad light curve with $\Delta m_{15} = 0.69$ but a normal luminosity, i.e., $M_V = -19.0$ mag. If a Δm_{15} correction is applied, the magnitude would be overcorrected by ~ 0.8 mag, i.e., roughly -18.5 mag, whereas the ΔC_{12} correction gives a more reasonable magnitude of -19.10 mag, much closer to the fiducial value: $M_V \approx -19.25$ for SN 1992al. Note that the ΔC_{12} method, at present, is still an officially empirical relation and more is needed to understand its underlying physics, e.g., the well-behaved opacity in the expanding fireball.

The Hubble diagrams in U , B , V , and I are displayed for 73 Hubble flow SNe Ia using the fully corrected apparent magnitudes. Solutions for the zero point α of the Hubble line are given for various subsets with different restrictions. We first inspected the velocity restriction. The Hubble diagram constructed by the two subsets, with different velocities demarcated at $v = 7000 \text{ km s}^{-1}$ but comparable sizes of the SN sample, shows little variation in α -values and the scatters. Inspections of the reddening restriction suggest that the α -values are also insensitive to the accepted maximum value of a host galaxy reddening. The uncertainties caused by the absorption correction were found to be $\lesssim 0.08$ mag in BVI , which justifies the reliability of our adopted absorption correction for SNe Ia. We finally examined the effect of the peculiar SNe Ia on the Hubble line. After ΔC_{12} correction, the larger luminosity difference between the normal SNe Ia and the peculiar ones has been narrowed down to ± 0.15 mag. Inclusion of a fraction of $\lesssim 20\%$ peculiar SNe Ia in the Hubble diagram will not significantly change the Hubble line.

With Cepheid distances to 11 nearby SNe Ia, including two peculiar ones, SN 1991T and SN 1999by, we have calibrated the

absolute magnitudes of SNe Ia and found the fully corrected mean value: $M_U^0 = -19.89 \pm 0.08$, $M_B^0 = -19.33 \pm 0.06$, $M_V^0 = -19.27 \pm 0.05$, and $M_I^0 = -18.97 \pm 0.04$. The forthcoming observations of SN 2006X in M100 (NGC 4321, which has a Cepheid distance; see Freedman et al. 2001) will further improve the determinations of the absolute magnitudes of SNe Ia. Applying the above calibration value to the Hubble flow SNe Ia, we derived the Hubble constant to be 72 ± 6 (total) $\text{km s}^{-1} \text{Mpc}^{-1}$. This value seems to be more robust and does not change with various combinations of distant SNe Ia and nearby calibrators. Reducing the uncertainty in the Hubble constant relies on a better understanding of the Cepheid P - L relation, the metallicity cor-

rection, and, more importantly, a more precise estimate of the distance to the LMC.

This work has been supported by the National Science Foundation of China (grants 10303002), the Basic Research Funding at Tsinghua University (JCqn2005036), and the National Key Basic Research Science Foundation (NKBRFSF TG199075402). We thank the referee for a number of critical comments and suggestions that helped us to improve the paper. We are grateful to Weidong Li for allowing us to use the data of SN 2002el before publication.

REFERENCES

- Altavilla, G., et al. 2004, *MNRAS*, 349, 1344
 Anupama, G. C., Sahu, D. K., & Jose, J. 2005, *A&A*, 429, 667
 Ardeberg, A., & de Groot, M. 1973, *A&A*, 28, 295
 Astier, P., et al. 2006, *A&A*, 447, 31
 Benetti, S., et al. 2004, *MNRAS*, 348, 261
 Branch, D. 1998, *ARA&A*, 36, 17
 Branch, D., Fisher, A., & Nugent, P. 1993, *AJ*, 106, 2383
 Branch, D., & Tammann, G. A. 1992, *ARA&A*, 30, 359
 Cristiani, S., et al. 1992, *A&A*, 259, 63
 de Vaucouleurs, G., de Vaucouleurs, A., Corwin, H. G., Jr., Buta, R. J., Paturel, G., & Fouque, P. 1991, *Third Catalogue of Bright Galaxies* (New York: Springer)
 Filippenko, A. V., et al. 1992a, *AJ*, 104, 1543
 ———. 1992b, *ApJ*, 384, L15
 Fiorentino, G., Caputo, F., Marconi, M., & Musella, I. 2002, *ApJ*, 576, 402
 Freedman, W. L., et al. 2001, *ApJ*, 553, 47
 Garnavich, P., et al. 2004, *ApJ*, 613, 1120
 Gibson, B. K., et al. 2000, *ApJ*, 529, 723
 Goldhaber, G., et al. 2001, *ApJ*, 558, 359
 Guy, J., Astier, P., Nobili, S., Regnault, N., & Pain, R. 2005, *A&A*, 443, 781
 Hamuy, M., Phillips, M. M., Suntzeff, N. B., Schommer, R. A., Maza, J., & Aviles, R. 1996a, *AJ*, 112, 2391
 ———. 1996b, *AJ*, 112, 2398
 Hamuy, M., Trager, S. C., Pinto, P. A., Phillips, M. M., Schommer, R. A., Ivanov, V., & Suntzeff, N. B. 2000, *AJ*, 120, 1479
 Hamuy, M., et al. 1996c, *AJ*, 112, 2408
 Henry, R. B. C., & Worthey, G. 1999, *PASP*, 111, 919
 Hoefflich, P., Wheeler, J. C., & Thielemann, F. K. 1998, *ApJ*, 495, 617
 Howell, A., & Nugent, P. 2004, in *Cosmic Explosions in Three Dimensions: Asymmetries in Supernovae and Gamma-Ray Bursts*, ed. P. Hoefflich, P. Kumar, & J. C. Wheeler (Cambridge: Cambridge Univ. Press), 151
 Ivanov, V. D., Hamuy, M., & Pinto, P. 2000, *ApJ*, 542, 588
 Jha, S. 2002, Ph.D. thesis, Harvard Univ.
 Jha, S., Branch, D., Chornock, R., Foley, R. J., Li, W., Swift, B. J., Casebeer, D., & Filippenko, A. V. 2006a, *AJ*, 132, 189
 Jha, S., et al. 1999, *ApJS*, 125, 73
 ———. 2006b, *AJ*, 131, 527
 Kennicutt, R., Jr., et al. 1998, *ApJ*, 498, 181
 Krisciunas, K., Prieto, J. L., Garnavich, P. M., Riley, J.-L. G., Rest, A., Stubbs, C., & McMillan, R. 2006, *AJ*, 131, 1639
 Krisciunas, K., et al. 2001, *AJ*, 122, 1616
 ———. 2003, *AJ*, 125, 166
 ———. 2004a, *AJ*, 127, 1664
 ———. 2004b, *AJ*, 128, 3034
 Leibundgut, B. 2000, *A&A Rev.*, 10, 179
 Leibundgut, B., et al. 1993, *AJ*, 105, 301
 Lentz, E. J., Baron, E., Branch, D., Hauschildt, P. H., & Nugent, P. E. 2000, *ApJ*, 530, 966
 Li, W., Filippenko, A. V., Treffers, R. R., Riess, A. G., Hu, J., & Qiu, Y. 2001a, *ApJ*, 546, 734
 Li, W., et al. 2001b, *PASP*, 113, 1178
 ———. 2003, *PASP*, 115, 453
 Li, W. D., et al. 1999, *AJ*, 117, 2709
 Lira, P. 1995, M.S. thesis, Univ. Chile
 Lira, P., et al. 1998, *AJ*, 115, 234
 Macri, L. M., Stetson, P. B., Bothun, G. D., Freedman, W. L., Garnavich, P. M., Jha, S., Madore, B. F., & Richmond, M. W. 2001, *ApJ*, 559, 243
 Madore, B. F., & Freedman, W. L. 1991, *PASP*, 103, 933
 Misra, K., Kamble, A. P., Bhattacharya, D. B., & Sagar, R. 2005, *MNRAS*, 360, 662
 Modjaz, M., Li, W., Filippenko, A. V., King, J. Y., Leonard, D. C., Matheson, T., Treffers, R. R., & Riess, A. G. 2001, *PASP*, 113, 308
 Nugent, P., Kim, A., & Perlmutter, S. 2002, *PASP*, 114, 803
 Parodi, B. R., Saha, A., Sandage, A., & Tammann, G. A. 2000, *ApJ*, 540, 634
 Patat, F., Benetti, S., Cappellaro, E., Danziger, I. J., della Valle, M., Mazzali, P. A., & Turatto, M. 1996, *MNRAS*, 278, 111
 Perlmutter, S., et al. 1997, *ApJ*, 483, 565
 ———. 1999, *ApJ*, 517, 565
 Phillips, M. M. 1993, *ApJ*, 413, L105
 Phillips, M. M., Lira, P., Suntzeff, N. B., Schommer, R. A., Hamuy, M., & Maza, J. 1999, *AJ*, 118, 1766
 Phillips, M. M., Wells, L. A., Suntzeff, N. B., Hamuy, M., Leibundgut, B., Kirshner, R. P., & Foltz, C. B. 1992, *AJ*, 103, 1632
 Phillips, M. M., et al. 1987, *PASP*, 99, 592
 ———. 2006, *AJ*, 131, 2615
 Pierce, M. J., & Jacoby, G. H. 1995, *AJ*, 110, 2885
 Pignata, G., et al. 2004, *MNRAS*, 355, 178
 Reindl, B., Tammann, G. A., Sandage, A., & Saha, A. 2005, *ApJ*, 624, 532 (R05)
 Richmond, M. W., et al. 1995, *AJ*, 109, 2121
 Riess, A. G., Press, W. H., & Kirshner, R. P. 1996a, *ApJ*, 473, 88
 ———. 1996b, *ApJ*, 473, 588
 Riess, A. G., et al. 1998, *AJ*, 116, 1009
 ———. 1999, *AJ*, 117, 707
 ———. 2004, *ApJ*, 607, 665
 ———. 2005, *ApJ*, 627, 579
 Saha, A., Sandage, A., Labhardt, L., Tammann, G. A., Macchetto, F. D., & Panagia, N. 1996, *ApJS*, 107, 693
 ———. 1997, *ApJ*, 486, 1
 Saha, A., Sandage, A., Tammann, G. A., Dolphin, A. E., Christensen, J., Panagia, N., & Macchetto, F. D. 2001a, *ApJ*, 562, 314
 Saha, A., Sandage, A., Tammann, G. A., Labhardt, L., Macchetto, F. D., & Panagia, N. 1999, *ApJ*, 522, 802
 Saha, A., Sandage, A., Thim, F., Labhardt, L., Tammann, G. A., Christensen, J., Panagia, N., & Macchetto, F. D. 2001b, *ApJ*, 551, 973
 Saha, A., Thim, F., Tammann, G. A., Reindl, B., & Sandage, A. 2006, *ApJ*, in press (astro-ph/0602572)
 Sahu, D. K., Anupama, G. C., & Prabhu, T. P. 2006, *MNRAS*, 366, 682
 Sakai, S., Ferrarese, L., Kennicutt, R. C., Jr., & Saha, A. 2004, *ApJ*, 608, 42
 Salvo, M. E., Cappellaro, E., Mazzali, P. A., Benetti, S., Danziger, I. J., Patat, F., & Turatto, M. 2001, *MNRAS*, 321, 254
 Sandage, A., Tammann, G. A., Saha, A., Reindl, B., Macchetto, F. D., & Panagia, N. 2006, *ApJ*, submitted (astro-ph/0603647)
 Schaefer, B. E. 1994, *ApJ*, 426, 493
 ———. 1995, *ApJ*, 449, L9
 ———. 1998, *ApJ*, 509, 80
 Schlegel, D. J., Finkbeiner, D. P., & Davis, M. 1998, *ApJ*, 500, 525
 Sebo, K. M., et al. 2002, *ApJS*, 142, 71
 Spergel, D. N., et al. 2003, *ApJS*, 148, 175
 Stritzinger, M., et al. 2002, *AJ*, 124, 2100
 Strolger, L.-G., et al. 2002, *AJ*, 124, 2905
 Tanvir, N. R., Ferguson, H. C., & Shanks, T. 1999, *MNRAS*, 310, 175
 Tonry, J. L., et al. 2003, *ApJ*, 594, 1
 Tripp, R. 1997, *A&A*, 325, 871
 Tripp, R., & Branch, D. 1999, *ApJ*, 525, 209
 Turatto, M., Piemonte, A., Benetti, S., Cappellaro, E., Mazzali, P. A., Danziger, I. J., & Patat, F. 1998, *AJ*, 116, 2431
 Turner, A., et al. 1998, *ApJ*, 505, 207
 Udalski, A., Soszynski, I., Szymanski, M., Kubiak, M., Pietrzynski, G., Wozniak, P., & Zebrun, K. 1999, *Acta Astron.*, 49, 223

- Umeda, H., Nomoto, K., Kobayashi, C., Hachisu, I., & Kato, M. 1999, *ApJ*, 522, L43
- Valentini, G., et al. 2003, *ApJ*, 595, 779
- Vazdekis, A., Peletier, R. F., Beckman, J. E., & Vasuso, E. 1997, *ApJS*, 111, 203
- Vinko, J., et al. 2003, *A&A*, 397, 115
- Wang, L. 2005, *ApJ*, 635, L33
- Wang, L., Goldhaber, G., Aldering, G., & Perlmutter, S. 2003, *ApJ*, 590, 944
- Wang, L., Höflich, P., & Wheeler, J. C. 1997, *ApJ*, 483, L29
- Wang, L., Strovink, M., Conley, A., Goldhaber, G., Kowalski, M., Perlmutter, S., & Siegrist, J. 2006, *ApJ*, 641, 50
- Wang, X., Wang, L., Zhou, X., Lou, Y.-Q., & Li, Z. 2005, *ApJ*, 620, L87
- Wells, L. A., et al. 1994, *AJ*, 108, 2233
- Worthey, G. 1994, *ApJS*, 95, 107
- Zehavi, I., Riess, A. G., Kirshner, R. P., & Dekel, A. 1998, *ApJ*, 503, 483